NASA TECHNICAL NOTE

NASA TN D-3550

NASA TN D-3550

AN ANALYSIS OF SUPERSONIC FLOW PHENOMENA IN CONICAL NOZZLES BY A METHOD OF CHARACTERISTICS

by Linwood B. Callis

Langley Research Center
Langley Station, Hampton, Va.

NATIONAL AERONAUTICS AND SPACE ADMINISTRATION • WASHINGTON, D. C. • AUGUST 1966

AN ANALYSIS OF SUPERSONIC FLOW PHENOMENA IN CONICAL NOZZLES BY A METHOD OF CHARACTERISTICS

By Linwood B. Callis

Langley Research Center
Langley Station, Hampton, Va.

NATIONAL AERONAUTICS AND SPACE ADMINISTRATION

For sale by the Clearinghouse for Federal Scientific and Technical Information
Springfield, Virginia 22151 – Price $2.00

AN ANALYSIS OF SUPERSONIC FLOW PHENOMENA IN CONICAL NOZZLES BY A METHOD OF CHARACTERISTICS

By Linwood B. Callis
Langley Research Center

SUMMARY

The method of axisymmetric irrotational characteristics is used in the analysis of the supersonic and hypersonic flow of a calorically perfect gas through conical nozzles. Solutions determine the Mach number, flow angularity, and stream function throughout the flow field in addition to the nozzle lengths and cone half-angles required for the expansion of the flow to a given center-line Mach number.

Calculations carried out for a wide range of inlet Mach numbers and cone half-angles allow, as in previous work, the prediction and explanation of the formation of oblique shock waves within the started nozzle. By using a characteristics method, shock-free solutions are obtained with minimum distortion of the conical profile. Typical Mach number contours with shock waves eliminated are shown.

An evaluation of the commonly made one-dimensional-flow assumption as applied to conical nozzles is made, and it is shown that significant errors may be present.

Finally, the existence of regions in which the flow properties prove to be independent of changes in the cone half-angle is pointed out and its importance is described and discussed.

INTRODUCTION

Currently, at Langley Research Center, much effort is being devoted to a study of basic modifications of the expansion tube as described in reference 1. Among the modifications considered, the one most likely to gain acceptance appears to be the expansion tunnel (ref. 2), a device utilizing a scoop-type conical nozzle to expand flows at relatively high Mach numbers (between 2 and 20) to even higher Mach number test conditions. To carry out the analysis of such a device, it was necessary that some means of accurately predicting the perfect-gas flow properties through the conical nozzles be available. The commonly made assumptions of "one-dimensional" flow (ref. 3) were believed to be inadequate since, for high Mach numbers, the flow to be expanded may proceed along the center line for a large number of inlet radii past the nozzle entrance before interacting

with the initial steady-flow expansion characteristics. Obviously, under such circumstances, a one-dimensional analysis would prove to be inadequate, and possibly the cause of serious error.

As a result of these considerations, such flows were examined in a more detailed fashion allowing reasonably precise information to be extracted for purposes of design and analysis. To this end, the method of axisymmetric irrotational characteristics has been applied, yielding solutions for a wide range of nozzle half-angles and inlet Mach numbers.

In addition to the information expected of the resulting computer program, several effects were observed which were believed to be of particular interest. Among these were recognition of the fact that, for scoop nozzles with sharp corners, a portion of the expanded flow field is completely independent of the growth of a viscous layer along the nozzle wall and that a standing oblique shock system is present in the steady-flow nozzle. Such shock systems have been observed in reference 4 and their cause and a method of elimination discussed in reference 5. Observance of these effects in the present work prompted an extended analysis conducted to determine

(1) the practical value, if any, of the region of flow independent of viscous effects on the wall, and

(2) whether the shock system could be eliminated from sharp-cornered scoop nozzles with inlet Mach number greater than 2 without seriously altering the nozzle profile.

A discussion of these effects and the means of analysis is presented in the following sections.

SYMBOLS

A	exit-to-inlet area ratio
F(x)	general function of x
j,k,r	summation indices
ℓ,m	parameters defined in equations (A3)
M	Mach number
M_c	characteristics solution of Mach number

M_1	one-dimensional solution of Mach number
M_i	Mach number at nozzle inlet
R	inlet radius of nozzle
r	radial distance in spherical coordinates
x'	axial coordinate measured from nozzle inlet
x	nondimensional axial coordinates, x'/R
x_f	value of x on center line at beginning of region I
x_t	value of x on center line at termination of region I
y'	radial coordinate measured from center line
y	nondimensional radial coordinate, y'/R
V_r	radial component of velocity vector
V_ϕ	azimuthal component of velocity vector
V_θ	component of velocity vector in θ direction
γ	ratio of specific heats, 1.4 for present work
δ^*	boundary-layer displacement thickness
Δ_M	error parameters, $(M_C - M_1)/M_C$
ζ	parameter defined in equations (A3)
θ	flow angle, degrees
θ_I	wall angle at nozzle corner, degrees
θ_v	wall angle at nozzle corner corrected for viscous effects (see eq. (3)), degrees

θ_{III} wall angle in region III, degrees

θ_{max} wall angle at inflection point, degrees

θ_w wall angle for source flow, degrees

$\mu = \sin^{-1}(1/M)$

ρ mass density

ϕ azimuthal angle in spherical coordinates

Subscripts:

A,B characteristic intersection at which properties are known

C characteristic point to be solved for

i conditions at nozzle inlet

max conditions at inflection point of nozzle wall

ref conditions at known reference point

A bar over a symbol indicates quantities averaged during iterative solution for a characteristic point.

ANALYSIS

The present investigation was carried out by using the well-known equations of change, derived in reference 6 and given in appendix A, along the characteristic lines. No general discussion of the equations, their derivation, or their application is included in the present work, inasmuch as a detailed discussion is given in reference 6.

Initially, the problem consisted of setting up a forward-computing characteristics solution for supersonic and hypersonic flows through conical nozzles. The inlet-flow Mach numbers and flow angularity were assumed to be known and the wall shape (conical) was specified. Figure 1 illustrates the general configuration, nomenclature, and the coordinate system used, the origin of which is taken on the center line at the nozzle entrance.

Input required for such a forward-computing characteristics solution consists of the specification of values of x, y, θ, μ, and M along the leading expansion characteristic from the corner to the center line and the Prandtl-Meyer conditions at the sharp nozzle corner. With the specification of the required input, the characteristics solution may then proceed downstream, flow properties being determined at the intersection of first-family with second-family characteristics.

Since the validity of the characteristics solutions depends in part upon the choice of variables, the mesh size used, and the means of determining higher order effects, it was desired to test the reliability of the present solutions by solving numerically a flow system for which exact solutions can be determined. For this purpose, solutions to source or radial flow were generated with the present program.

Properties of the source flow field, depending solely on the radial distance from the designated source, may be analytically described simply by a consideration of the compressible continuity equation written in spherical coordinates together with the isentropic flow relations. Derivation of the governing field equations for this flow is presented in appendix B as well as the equations necessary to determine, for program input purposes, the shape of and properties along the leading characteristic. Results of this comparison are shown in figure 2 for source flow with a beginning Mach number at the wall of 2.0 and $\theta_w = 5.0^o$. Agreement with theory in all check cases was excellent.

It was believed at this point that solutions to the conical nozzle problem could be generated with confidence. However, when these solutions were attempted, it was determined that characteristics of like family intersected near the center line, suggesting the existence of an oblique shock wave (as observed in ref. 4) lying just downstream of the corner expansion. Sketch 1 indicates this phenomenon, and Mach number contours are shown in figure 3 for a typical case in which this effect was observed. These Mach number contours, coupled with observed regions of negatively inclined flow near the center line and regions of flow more positively inclined than the wall angle serve both to confirm and to indicate the necessity of an oblique shock structure in this position.

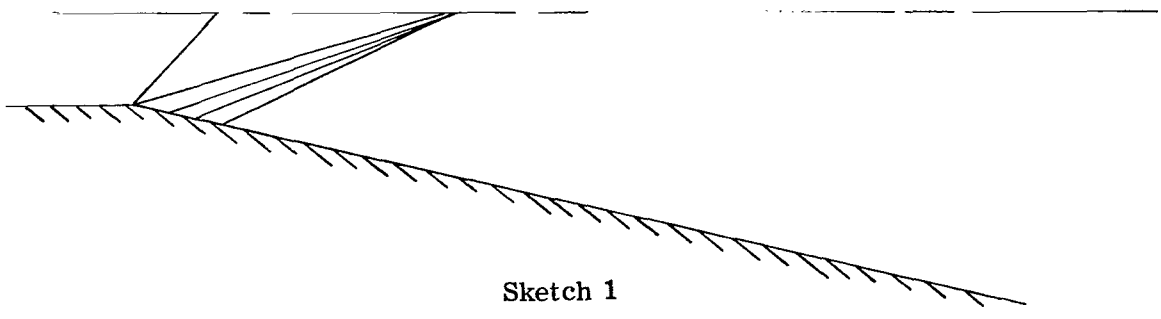

Sketch 1

At this point, every effort was made to make certain that the observed effects were not due to the particular inlet condition, wall angle, characteristics mesh size, or computing errors. Therefore, a large number of cases were run which encompassed a variation of these parameters. In each case, the computing sequence was checked in detail and, in each, the converging of the characteristics was present. It was concluded that the physical presence of a weak shock system, also reported in references 4 and 5, was the cause of the difficulty and that the flow problem as posed could not be solved by means of the irrotational system of characteristics.

Two alternatives presented themselves: Analyze the system, including the discontinuous structure or determine numerically the shape of a transition section, eliminating the shock, yet allowing a conical nozzle to be attached immediately downstream of this section. The second alternative was chosen.

The problem as posed at this point consisted of determining the shape of a transition region required to eliminate the observed compression characteristics. In order to accomplish this, the flow field was divided into three computational regions as shown in figure 4.

Region I consists of the flow field embraced by the corner rays. This portion of the flow was determined to be free of compression characteristics and computations were carried out as originally intended. Though a rigorous determination of the envelope of intersecting characteristics would shift the beginning of region II slightly upstream, it is believed that the shift would not be sufficient to affect the flow in region I. Hence this effect was ignored.

It is within region II that the observed compressions are eliminated. This elimination is accomplished by restricting the center-line Mach number in region II to the last determined value in region I and thus eliminating the possibility of a shock. This specification of the center-line Mach number, coupled with a solution in region I, permits the flow of characteristic computations (indicated by arrows in fig. 4) to be reversed and thus allows the determination of the wall shape required to insure such a flow configuration.

With such a computation scheme in region II, it may be expected that the wall angle will initially vary in a fashion such that the flow exiting from region I will be further expanded and will allow elimination of the troublesome intersecting characteristics. However, to satisfy continuity relationships, it can be argued that maintaining a constant center-line Mach number in region II will require that an inflection point and maximum wall angle be present past which the wall angle grows progressively smaller until it reaches zero and the flow across the entire cross section has constant properties. It is at, or downstream of, the inflection point that region II may be safely terminated by attaching a conical nozzle with a half-angle equal to the local wall angle.

At this point, a word of explanation is offered with regard to the determination of wall-point conditions in region II. Normally, when the center-line Mach number is specified, wall contours are determined by evaluating properties along a characteristic line from the center line toward the wall until continuity requirements are satisfied. This procedure, however, implies an upstream movement from one characteristic to the next, the reverse of the present situation illustrated in sketch 2.

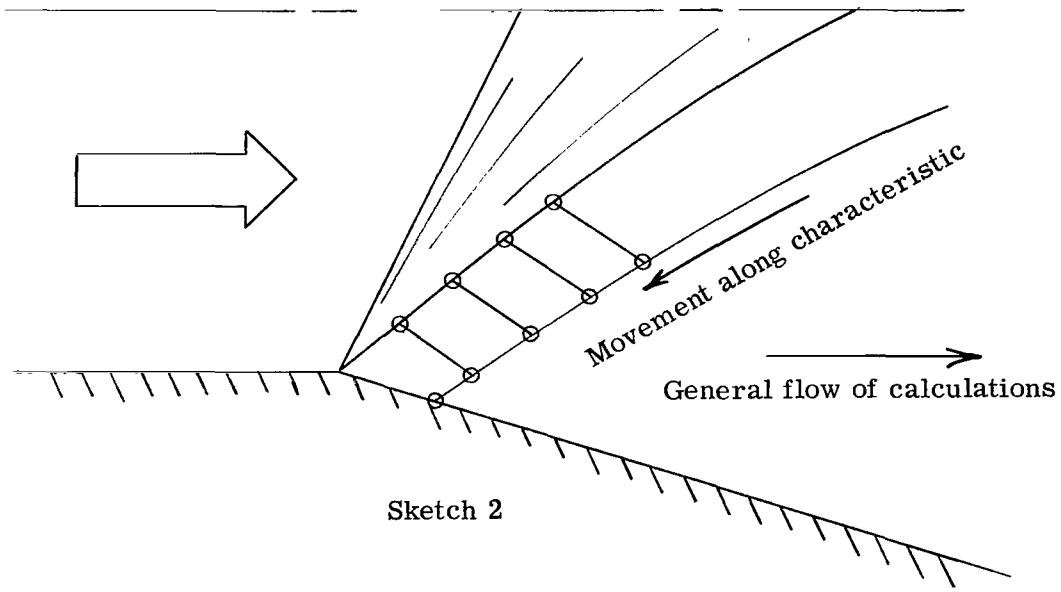

Sketch 2

Hence, this means of determining the wall contour cannot be used. Instead, the predetermined center-line Mach number in region II and the solutions along the preceding characteristic are used to determine solutions for properties along the characteristic in question at all points except the wall point. Values of M and θ at the wall point (the coordinates of which are simply determined) cannot be determined with the equation of change (eq. (A1)) since, without interpolating, only one equation is available to solve for the two flow conditions. Various methods are available for determining the flow variables at this wall point, all involving either interpolation or extrapolation. Recourse in this instance is made to a Lagrangian extrapolation of M and θ, along the characteristic of interest, to the wall by utilizing a fourth-degree-polynomial fit. The relation yielding such a fit to a function $F(x)$ is

$$F(x) = \sum_{k=0}^{n} F(x_k) \prod_{\substack{j=0 \\ j \neq k}}^{n} \left(\frac{x - x_j}{x_k - x_j} \right) \tag{1}$$

the indexed values of x being the points at which the function is known. With the five known points immediately preceding the wall point (shown in sketch 2) equation (1) may be used to evaluate M and θ at the wall. This extrapolation, carried out along a characteristic of the first family in terms of x, extends one mesh spacing or less and is believed to be quite accurate. Computations proceed in this fashion until the wall inflection point is reached or until a specific local wall angle (less than the maximum wall angle) downstream of the inflection point is reached.

In region III, the direction of computation along the characteristics is once again reversed and the solution, with the wall shape specified, is continued to completion. Such a computational scheme, programed for an electronic computer, was found to be successful in removing shocks from conical nozzles. Similar methods were used in reference 5. Typical Mach number contours for such a shock-free nozzle are indicated in figure 5 for a uniform parallel flow of $M_i = 2.0$ entering a nozzle with an initial wall angle of 9.58°. The solution indicates that, at the end of the transition section, a maximum wall angle of 15.15° is reached, this being taken as the half-angle of the attached conical nozzle. Further, Mach number contours illustrate the existence of a rhombus of parallel constant-property flow resulting from the specification of an invariant center-line Mach number with region II. Downstream of this rhombus, contours smooth out and approach the spherical-cap source flow profiles (fig. 2(b)) to which they must tend in the limit. (Further discussion of this flow configuration is presented in a subsequent section.)

RESULTS AND DISCUSSION

Region I

Numerical solutions to the present problem indicate that in region I no converging or compression characteristics are present. This is both expected and easily understood since in this flow region no effects of the wall contour are manifested, the expansion being generated solely by the flow around the sharp corner. Shown in figure 6 is a composite analysis of the center-line flow within region I. Presented are the axial distance x_t for a given M_i and θ_I, at which this region terminates and the observed shock occurs. Cross-plotted are values of Mach number reached during this expansion and immediately prior to the shock.

The upstream limit of region I, x_f, is given by the expression

$$x_f = \sqrt{M_i^2 - 1} \tag{2}$$

for uniform entering flow and is the number of radii the center-line flow must travel past the nozzle inlet before the flow expansion actually begins. Clearly, to this point in the

nozzle, use of a one-dimensional approximation is in error because the center-line flow has not "sensed" the presence of the nozzle. Errors of this nature are more severe for configurations having high inlet Mach numbers such as those anticipated in expansion-tunnel operation.

Also interesting is the relative expansion effectiveness of a given corner turn in an axisymmetric nozzle as compared to a wedge-type (two-dimensional) nozzle. Figure 6 indicates that, for $M_i = 5$ and $\theta_I = 10^o$, the terminal Mach number, generated by the expansion from the corner, is 35 on the center line. In two dimensions, the same entrance conditions and corner turning angle result in a terminal Mach number of 8.83. Though such a trend is expected from area-ratio considerations, the magnitude of the difference is startling.

At this point, one is inclined to speculate on the possible advantages of using an axisymmetric corner expansion rather than conventional nozzles for the purpose of generating hypersonic flows. First, however, the similarity between this type of expansion process and the minimum-length nozzle expansion should be commented upon. In both, all expansion characteristics are generated at the sharp inlet corner of the nozzle. The minimum-length nozzle is then contoured so that these characteristics, having been traversed by the flow, are canceled, uniform flow being established at the nozzle exit. The major disadvantage of such a nozzle is that, due to viscous effects, it operates primarily at one design point, and attempts to utilize the nozzle at other than design conditions result in incomplete cancellation, possibly prohibitive.

In order to circumvent such difficulties, the axisymmetric corner expansion with no cancellation may be used, provided the resultant flow gradients in region I are tolerable. In this connection, figures 7 and 8 present, respectively, contours of constant M and θ in region I as well as the transverse extent of region I (dashed lines) as determined by values of M_i and θ_I. It is clear from figure 7 that, for values of $M \geqq 20$, only small transverse variations of M occur near the center line ($y \leqq 1$) for $2 \leqq M_i \leqq 20$. The extent of the region in which this is true is determined by the particular values of M_i and θ_I under consideration. Figure 8, presenting contours of constant θ, indicates that for $x \geqq 30$ the transverse variation of θ near the center line is essentially that of source flow for the M_i considered here. Clearly, as M_i decreases and M increases, the approximation of these gradients by source flow gradients becomes more valid and the region over which the approximation can be made becomes larger. Hence, the corner expansion provides a flow with essentially source flow gradients with an expansion to the desired M in the minimum possible length. In addition, since the flow in region I is insensitive to the wall contour, the wall may be diverted in such a way as to insure that viscous effects on the center-line flow are minimized. In fact, in a shock or expansion tube, if the nozzle inlet is used as a scoop expanding (as in the present work) only the uniform "inviscid core" of the oncoming flow, viscous effects can be constrained

to a modification of the corner half-angle by an amount $\tan^{-1}(\cos \theta_I \, d\delta^*/dx)$ due to the initial growth of the displacement thickness at the sharp leading edge. In this connection, the relationship between θ_I and θ_v is given by

$$\theta_v = \theta_I - \tan^{-1}(\cos \theta_I \, d\delta^*/dx) \tag{3}$$

the two angles being identical for inviscid flow. All computations presented herein are for inviscid flow.

Two more points, flow invariance and error due to one-dimensional approximations, should be noted. For a given inlet Mach number, increasing the corner angle a given amount simply extends the flow expansion in region I, leaving completely unchanged the flow established by the original corner. This is, of course, advantageous in that large-angle solutions for given inlet Mach numbers encompass all small-angle solutions. Therefore, from a practical viewpoint, flow generated by lower values of θ_I is unaffected by viscous fluctuations (see eq. (3)) in the turning angle as long as these fluctuations occur at higher values of θ_I. Consequently, if θ_I is made large enough to provide a cushion against such fluctuations, viscous effects may be removed from the test entirely as indicated in sketch 3.

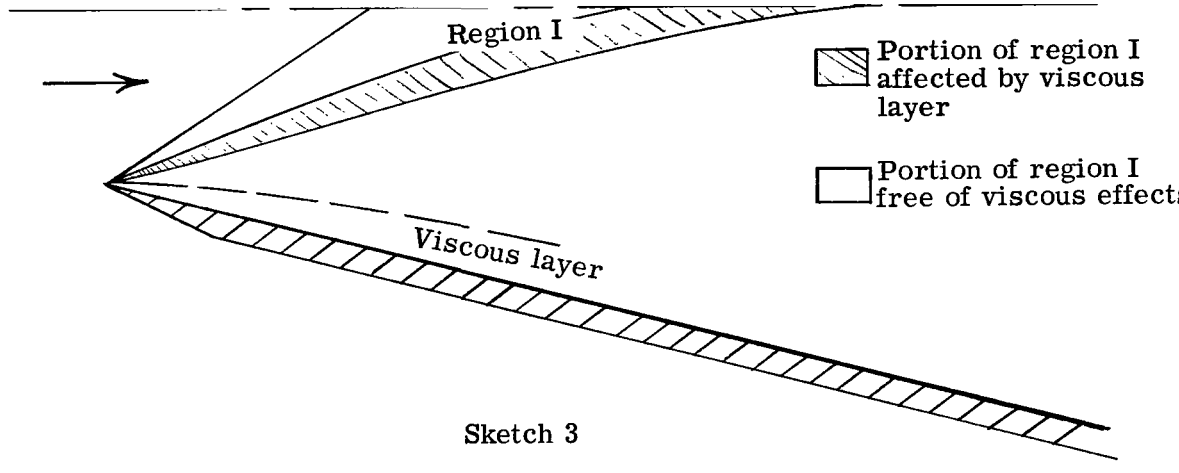

Sketch 3

The prediction of the center-line flow in region I is best accomplished with the aid of numerical solutions presented in figure 6 rather than approximate one-dimensional methods. One-dimensional assumptions lead to errors in the predicted center-line Mach number, an indication of this error being the parameter $\Delta_M = \dfrac{M_c - M_1}{M_c}$ shown in figure 9 as a function of A, θ_I, and M_i. As seen in figure 9, these errors can be significant (up to 60 percent), with M_1 having values both above and below M_c.

Values of $M_1 > M_c$ occur when the flow first enters the nozzle; a one-dimensional analysis predicts an immediate increase in M_1 when, in fact, the center-line Mach number remains constant for $M_i^2 - 1$ radii past the nozzle entrance. When the expansion is encountered, however, values of M_c increase more swiftly than values of M_1, eventually surpassing them. The one-dimensional theory now tends to underpredict the characteristics solution. Curves in figure 9 are shown only for region I (the corner expansion) and are terminated at the end of this region by dashed lines.

Region II

The first characteristics reflected from the wall converge to form a weak shock within region II near the center line. The formation of this shock wave is easily understood upon consideration of figure 10. This figure presents typical contours of constant flow inclination ($\theta = 3^\circ, 4^\circ, 5^\circ$, and 6°) for uniform flow entering a conical nozzle at $M_i = 1.5$ with $\theta_I = 4.14^\circ$ and no transition section attached. As previously mentioned, within region I some of the flow areas are inclined at angles larger than the conical wall angle. This flow must, by some wave mechanism, be turned back toward the center line. Since the expansion characteristics "reflected" from the center line are unable to accomplish this, the mechanism which develops is a compression generated by the first characteristics reflected from the wall processing the flow immediately after its exit from region I. The shock formation then is a reconciliation of an incompatibility between the flow at the exit of region I and the final wall angle reached at the sharp nozzle corner.

The cause of this overexpansion within region I may be traced to the terms $-l\frac{dx}{y}$ and $-m\frac{dx}{y}$ in the equations (A1) and (A2), respectively. These terms, which vanish in the two-dimensional solution, contribute in the axisymmetric solution for θ in such a fashion that along a corner-ray characteristic θ does not decrease monotonically from the corner value to a center-line value of zero. Rather, these terms, peculiar to axisymmetric flow, combine to drive θ to a maximum value (greater than the wall angle) from which it declines to zero at the center line.

Hence the shock, as pointed out in reference 5, is an axisymmetric effect not present in two-dimensional flows. It is due to the overexpanded flow coupled with a wall contour which does not permit the flow to be turned back toward the center line gradually. From these considerations, it is clear that shocks may be present in a variety of nozzles with a wide range of inlet Mach numbers and with contours which, though divergent, are specified arbitrarily. To avoid this situation, the present scheme has been used to determine a transition region necessary to prevent shock formation. As has been argued previously, there is, at the downstream end of this transition, an inflection point. Figures 11, 12, and 13 show, respectively, values of θ_{max}, x_{max}, and y_{max} at this point as a

function of θ_I and M_i. Figure 14 illustrates a typical transition profile required to prevent shocks from forming in a conical nozzle.

With values of θ_{max}, x_{max}, and y_{max} available, it was believed that the entire family of transition profiles could be easily represented by a fourth-degree polynomial of the form

$$y = \sum_{r=0}^{4} C_r x^r \tag{4}$$

where, with known conditions at the inflection point and sharp corner, the equations for C_i are determined to be

$$\left.\begin{aligned} C_0 &= 1.0 \\ C_1 &= \tan \theta_I \\ C_2 &= \left[6(y_{max} - 1) - 3x_{max}(\tan \theta_I + \tan \theta_{max})\right] \frac{1}{x_{max}^2} \\ C_3 &= \left[-8(y_{max} - 1) + x_{max}(3 \tan \theta_I + 5 \tan \theta_{max})\right] \frac{1}{x_{max}^3} \\ C_4 &= \left[3(y_{max} - 1) - x_{max}(\tan \theta_I + 2 \tan \theta_{max})\right] \frac{1}{x_{max}^4} \end{aligned}\right\} \tag{5}$$

The circular symbols shown in figure 14 indicate points on the transition profile determined with the aid of equations (4) and (5) and data presented in figures 11 to 13. Transition profiles may easily be determined in this fashion, and it is believed that these profiles will result in shock-free flow.

The section on "Analysis" indicates that computations in region II may be stopped when the inflection point of the wall is reached. The program, however, is such that the calculations of the wall contour could be continued past the inflection point until any arbitrary wall angle, less than the value at the inflection point, is reached. Continuing the calculations until $\theta_I = 0$ results in a minimum-length contour with uniform flow over the entire cross section. This capability provides assurance that shock-free flow can be achieved in a nozzle having any desired wall angle. In addition, if testing within the rhombus of uniform flow is desired, the dimensions of this rhombus can be governed by extending region II past the wall inflection point. It is, in fact, the intersection of the rhombus with the nozzle wall that terminates the minimum-length-nozzle contour.

In light of these efforts to eliminate the predicted shock wave, it is natural to question the effect on the nozzle flow should the shock be allowed to develop. Weak disturbances (as the present shocks are assumed to be), though failing to separate the boundary layer, may cause perturbations in the expected flow quantities or a general increase in the entropy of the nozzle flow. These effects, which reduce nozzle efficiency, would be harmful in nozzles used with propulsive units. Such effects would render useless nozzles used in investigations in which a relatively precise knowledge of the chemical kinetics of the flow is required. In general, it is desirable to avoid shock formations in most nozzles with high flow velocity.

Wave formations such as those discussed and predicted in the present paper have not been observed experimentally to the author's knowledge. It is not certain whether this lack of verification is due to a lack of investigation or to a washing-out effect due to viscous effects. Since the flow adjacent to the wall experiences a decrease in the value of $\tan^{-1}(\cos \Theta_I \, d\delta^*/dx)$ as it progresses downstream, it is conceivable that δ^* varies in a fashion such that an effective fluid-dynamic contouring of the wall occurs and allows the overexpanded flow to adjust without the influence of a shock. These, however, are speculations of the author and warrant additional investigation with viscous effects accounted for.

Region III

Region III consists of the flow field determined by the conical wall "fitted" at the end of Region II. The flow in this region is relatively uninteresting, being shock free and approaching source flow profiles far downstream of the nozzle entrance. It can be argued on this basis that $\Delta_M \to 0$ as $x \to \infty$, the one-dimensional analysis (appendix B) now accurately predicting the flow profiles and quantities. A typical variation of Δ_M over all regions is presented in figure 15. The decrease of Δ_M noted in region II is due to the constancy of M_c within this region and the increase in M_1. In region III, Δ_M increases initially to a value slightly above zero and then begins its asymptotic approach to zero and purely one-dimensional flow.

CONCLUDING REMARKS

An analysis of supersonic flow phenomena for a calorically perfect gas in conical nozzles has been made by use of the method of axisymmetric irrotational characteristics. The following remarks are based on the results of this analysis:

(1) The present forward-computing characteristics solution provides a means of generating transition contours and evaluating the resulting shock-free flow. Provisions are made for fitting conical sections to the transition region or the contours may be extended to yield a minimum-length nozzle with uniform exiting flow.

(2) The assumption of one-dimensional flow in such nozzles is shown to be seriously in error in some flow regions.

(3) Provided source flow gradients can be tolerated, it is suggested that the axisymmetric expansion generated by a sharp corner is the most straightforward means of expanding a flow to high supersonic Mach numbers. In addition to achieving the desired conditions in the minimum downstream distance, these conditions can be made to be completely independent of both viscous effects and, within reason, the wall contour downstream of the sharp nozzle corner.

(4) Conical nozzles and other divergent but arbitrarily contoured nozzles are not necessarily free of shock formations caused by axisymmetric overexpansions in such flows.

Langley Research Center,
National Aeronautics and Space Administration,
Langley Station, Hampton, Va., April 28, 1966.

APPENDIX A

CHARACTERISTIC EQUATIONS

As briefly as possible, the basic irrotational axisymmetric characteristic equations used in this analysis are presented.

In differential form, the governing equations relating properties along a characteristic of the first family are

$$\left.\begin{aligned} \frac{dy}{dx} &= \tan(\theta + \mu) \\ \frac{dM}{\zeta M} - d\theta \tan \mu - l \frac{dx}{y} &= 0 \end{aligned}\right\} \tag{A1}$$

and for the second family are

$$\left.\begin{aligned} \frac{dy}{dx} &= \tan(\theta - \mu) \\ \frac{dM}{\zeta M} + d\theta \tan \mu - m \frac{dx}{y} &= 0 \end{aligned}\right\} \tag{A2}$$

where

$$\left.\begin{aligned} l &= \frac{\sin \mu \sin \theta \tan \mu}{\cos(\theta + \mu)} \\ m &= \frac{\sin \mu \sin \theta \tan \mu}{\cos(\theta - \mu)} \\ \zeta &= 1 + \frac{\gamma - 1}{2} M^2 \end{aligned}\right\} \tag{A3}$$

These equations, derived and presented in slightly different form in reference 6, may be cast in finite-difference form and the unknown properties solved for at the intersection of characteristics of the opposite family. Equations by which solutions are obtained at the various types of intersections are shown as follows:

For intersections at a general point:

$$x_C = \frac{y_B - y_A + x_A \tan\left(\bar{\theta}_A + \bar{\mu}_A\right) - x_B \tan\left(\bar{\theta}_B - \bar{\mu}_B\right)}{\tan\left(\bar{\theta}_A + \bar{\mu}_A\right) - \tan\left(\bar{\theta}_B - \bar{\mu}_B\right)} \tag{A4}$$

$$y_C = (x_C - x_A)\tan(\bar{\theta}_A + \bar{\mu}_A) + y_A \tag{A5}$$

$$\theta_C = \frac{\left\{ \begin{array}{l} M_B - M_A + \bar{\xi}_B \bar{M}_B \theta_B \tan \bar{\mu}_B + \bar{\xi}_A \bar{M}_A \theta_A \tan \bar{\mu}_A \\ + \dfrac{\bar{\xi}_B \bar{M}_B \bar{m}_B (x_C - x_B)}{\bar{y}_B} - \dfrac{\bar{\xi}_A \bar{M}_A \bar{l}_A (x_C - x_A)}{\bar{y}_A} \end{array} \right\}}{\bar{\xi}_B \bar{M}_B \tan \bar{\mu}_B + \bar{\xi}_A \bar{M}_A \tan \bar{\mu}_A} \tag{A6}$$

$$M_C = \bar{\xi}_A \bar{M}_A (\theta_C - \theta_A)\tan \bar{\mu}_A + \frac{\bar{\xi}_A \bar{M}_A \bar{l}_A (x_C - x_A)}{\bar{y}_A} + M_A \tag{A7}$$

For intersections at a wall point:

$$x_C = \frac{y_B - y_A + x_A \tan \theta_w - x_B \tan(\bar{\theta}_B - \bar{\mu}_B)}{\tan \theta_w - \tan(\bar{\theta}_B - \bar{\mu}_B)} \tag{A8}$$

$$y_C = (x_C - x_A)\tan \theta_w + y_A \tag{A9}$$

$$\theta_C = \theta_w \tag{A10}$$

$$M_C = \bar{\xi}_B \bar{M}_B (\theta_B - \theta_w)\tan \bar{\mu}_B + \frac{\bar{\xi}_B \bar{M}_B \bar{m}_B (x_C - x_B)}{\bar{y}_B} + M_B \tag{A11}$$

For intersections at a center-line point:

$$y_C = \theta_C = 0 \tag{A12}$$

$$x_C = x_A - \frac{y_A}{\tan(\bar{\theta}_A + \bar{\mu}_A)} \tag{A13}$$

M_C obtained from equation (A7)

For intersections one point off the center line:

x_C, y_C, and M_C obtained from equations (A4), (A5), and (A7), respectively

APPENDIX A

$$\theta_C = \frac{M_B - M_A + \bar{\xi}_A \bar{M}_A \theta_A \tan \bar{\mu}_A - \dfrac{\bar{\xi}_A \bar{M}_A \bar{l}_A (x_C - x_A)}{\bar{y}_A}}{\bar{\xi}_A \bar{M}_A \tan \bar{\mu}_A + 2\bar{\xi}_B \bar{M}_B \tan \bar{\mu}_B} \tag{A14}$$

Equations (A1) to (A14), being well known and frequently used, will not be discussed further either with regard to their derivation or their general application. It should, however, be pointed out that in the present solution, once first approximations of the unknown at C have been determined, second approximations that consider second-order terms are obtained by using the average of the values at A and C, or at B and C, for the inclination of the characteristic lines and for all values of quantities that appear in the coefficients of equations (A1) and (A2) (the barred quantities in eqs. (A4) to (A14)).

APPENDIX B

SOURCE FLOW

The properties of source flow pictured physically in the following sketch

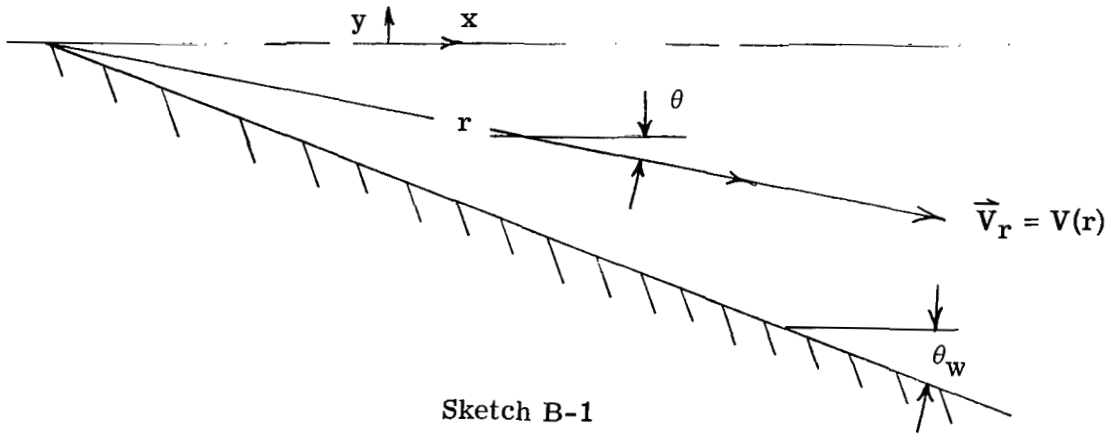

Sketch B-1

may be simply determined with the aid of the compressible continuity equation, written in spherical coordinates (r, θ, ϕ), which is

$$\frac{1}{r^2}\frac{\partial}{\partial r}\left(r^2 \rho V_r\right) + \frac{1}{r \sin\theta}\frac{\partial}{\partial \phi}\left(\rho V_\phi\right) + \frac{1}{r \sin\theta}\frac{\partial}{\partial \theta}\left(\rho V_\theta \sin\theta\right) = 0 \tag{B1}$$

Since for source flow $V_\theta = V_\phi = 0$, equation (B1) may be written

$$r^2 \rho V_r = \text{Constant} \tag{B2}$$

Evaluating the constant appearing in equation (B2) at some reference point (at which conditions are known) and applying the isentropic steady-flow relations yields the following implicit solution for M in terms of r:

$$\frac{M_{ref}}{M} = \left(\frac{1 + \frac{\gamma - 1}{2} M_{ref}^2}{1 + \frac{\gamma - 1}{2} M^2}\right)^{\frac{\gamma+1}{2(\gamma-1)}} \left(\frac{r}{r_{ref}}\right)^2 \tag{B3}$$

APPENDIX B

If the reference point is chosen so that it lies on the wall, or boundary of the flow, and has the Cartesian coordinates $x = 0$, $y = -1$, it follows that

$$\left.\begin{aligned} r_{ref} &= -(\sin \theta_w)^{-1} \\ x &= r \cos \theta + \cot \theta_w \\ y &= r \sin \theta \end{aligned}\right\} \tag{B4}$$

These equations allow the complete and exact specification of the source flow field.

In order to provide required input for the numerical solution of the source flow field, values of flow quantities must be known along a characteristic from the reference point to the center line. The slope of this characteristic is given as

$$\frac{dy}{dx} = \tan(\theta + \mu) \tag{B5}$$

If equation (B4) in differential form is substituted into (B5) the result may be written as

$$\frac{dr}{r} \tan \mu = d\theta \tag{B6}$$

Recognizing that $\tan \mu = (M^2 - 1)^{-1/2}$ and utilizing equation (B3) allows equation (B6) to be integrated in closed form to give

$$\theta - \theta_w = \frac{1}{2}\left[\sqrt{\frac{\gamma + 1}{\gamma - 1}} \tan^{-1}\sqrt{\frac{M^2 - 1}{(\gamma + 1)/(\gamma - 1)}} - \cos^{-1}\frac{1}{M}\right]\Bigg|_{M_{ref}}^{M} \tag{B7}$$

With equations (B3), (B4), and (B7) the leading characteristic is completely defined and the necessary input available.

REFERENCES

1. Trimpi, Robert L.: A Preliminary Theoretical Study of the Expansion Tube, A New Device for Producing High-Enthalpy Short-Duration Hypersonic Gas Flows. NASA TR R-133, 1962.

2. Trimpi, Robert L.; and Callis, Linwood B.: A Perfect-Gas Analysis of the Expansion Tunnel, A Modification to the Expansion Tube. NASA TR R-223, 1965.

3. Liepmann, H. W.; and Roshko, A.: Elements of Gasdynamics. John Wiley & Sons, Inc., c.1957.

4. Migdal, David; and Landis, Fred: Characteristics of Conical Supersonic Nozzles. ARS J., vol. 32, no. 12, Dec. 1962, pp. 1898-1901.

5. Migdal, D.; and Kosson, R.: Shock Predictions in Conical Nozzles. AIAA J. (Tech. Notes), vol. 3, no. 8, Aug. 1965, pp. 1554-1556.

6. Ferri, Antonio: Elements of Aerodynamics of Supersonic Flows. The Macmillan Co., 1949.

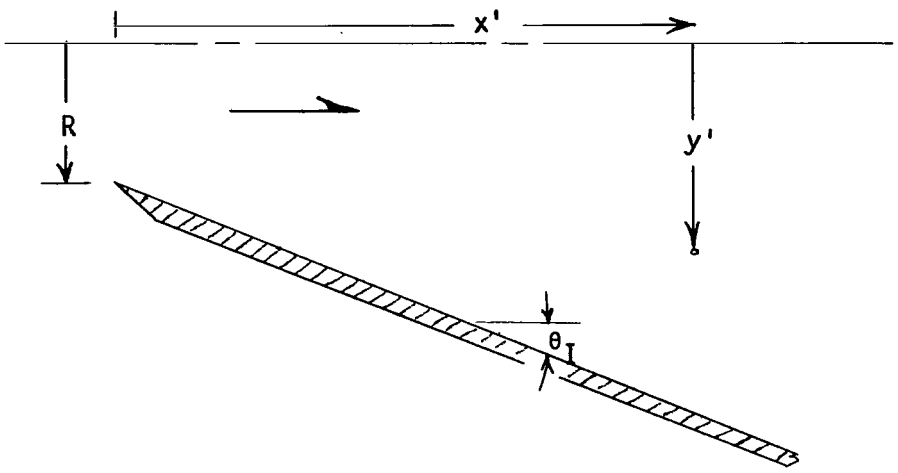

Figure 1.- General configuration and coordinate system for conical nozzle.

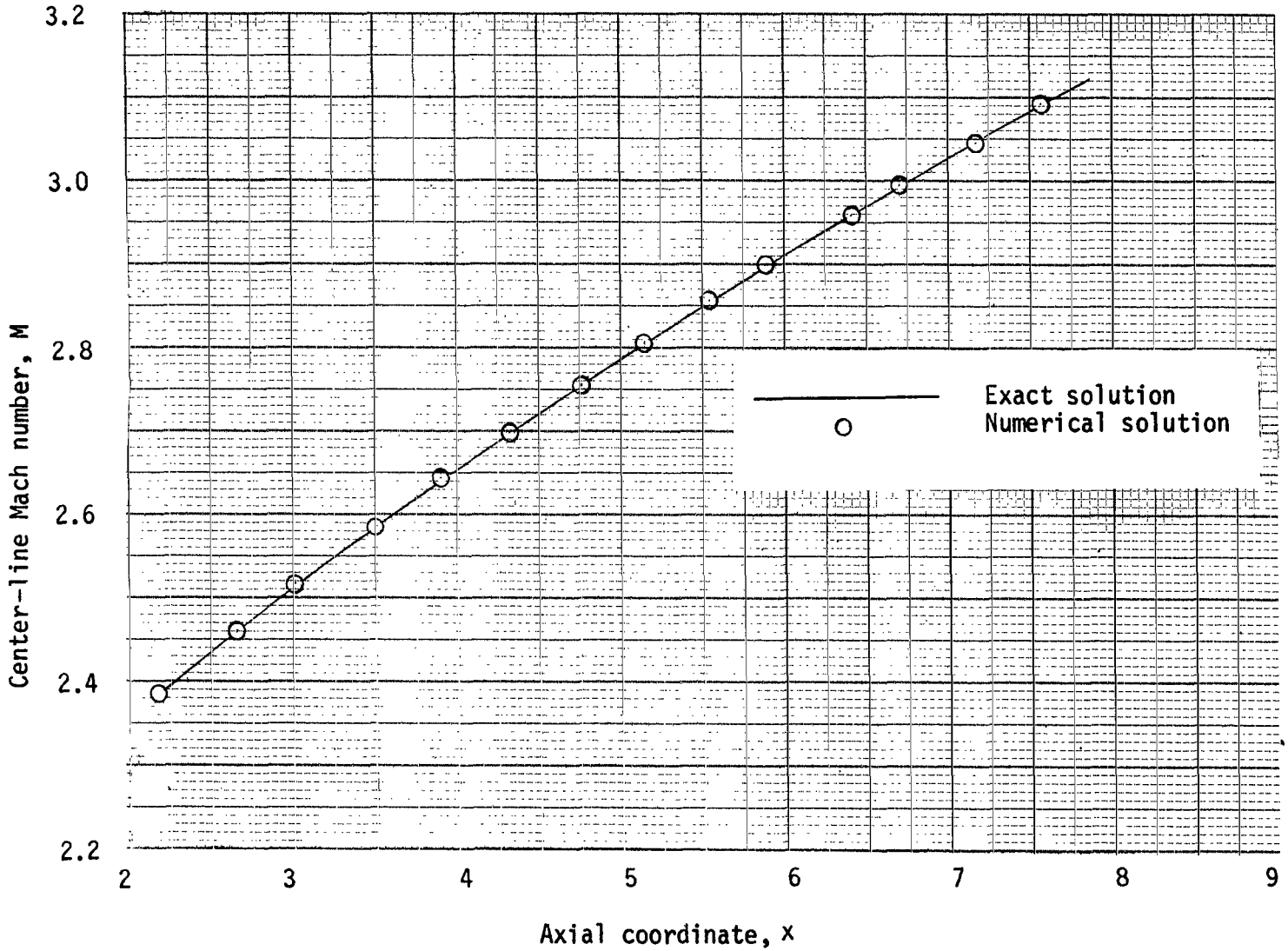

(a) Center-line Mach number.

Figure 2.- Exact and numerical source flow solutions for $\theta_w = 5.0^0$.

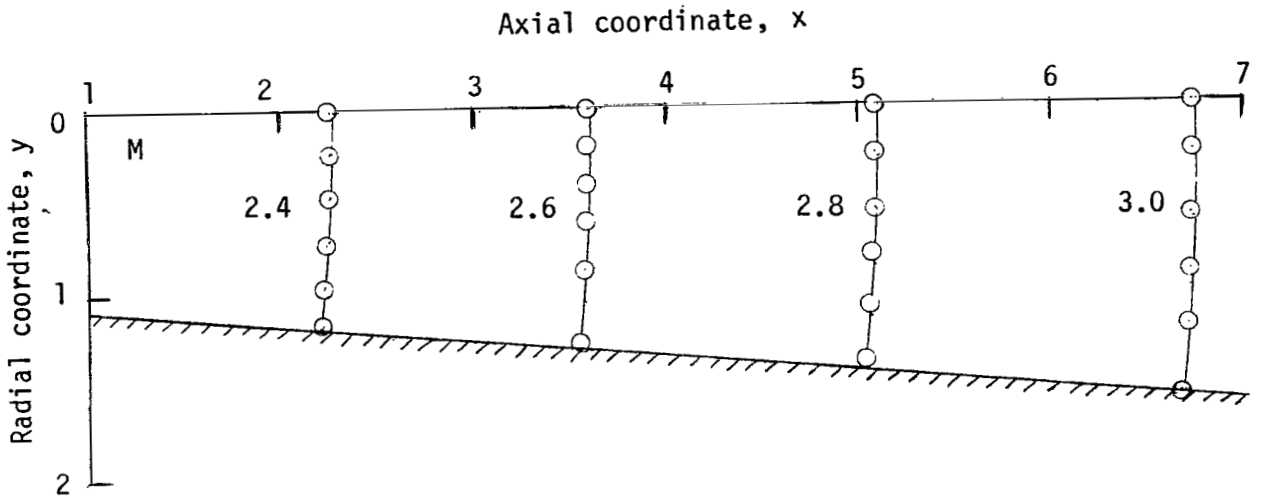

(b) Constant Mach number contours.

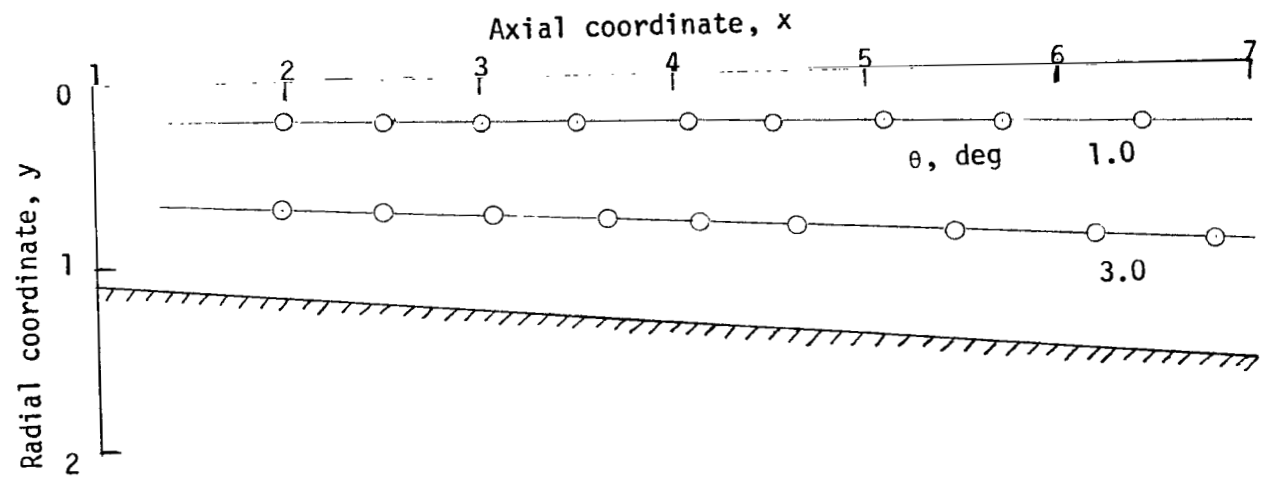

(c) Lines of constant flow inclination.

Figure 2.- Concluded.

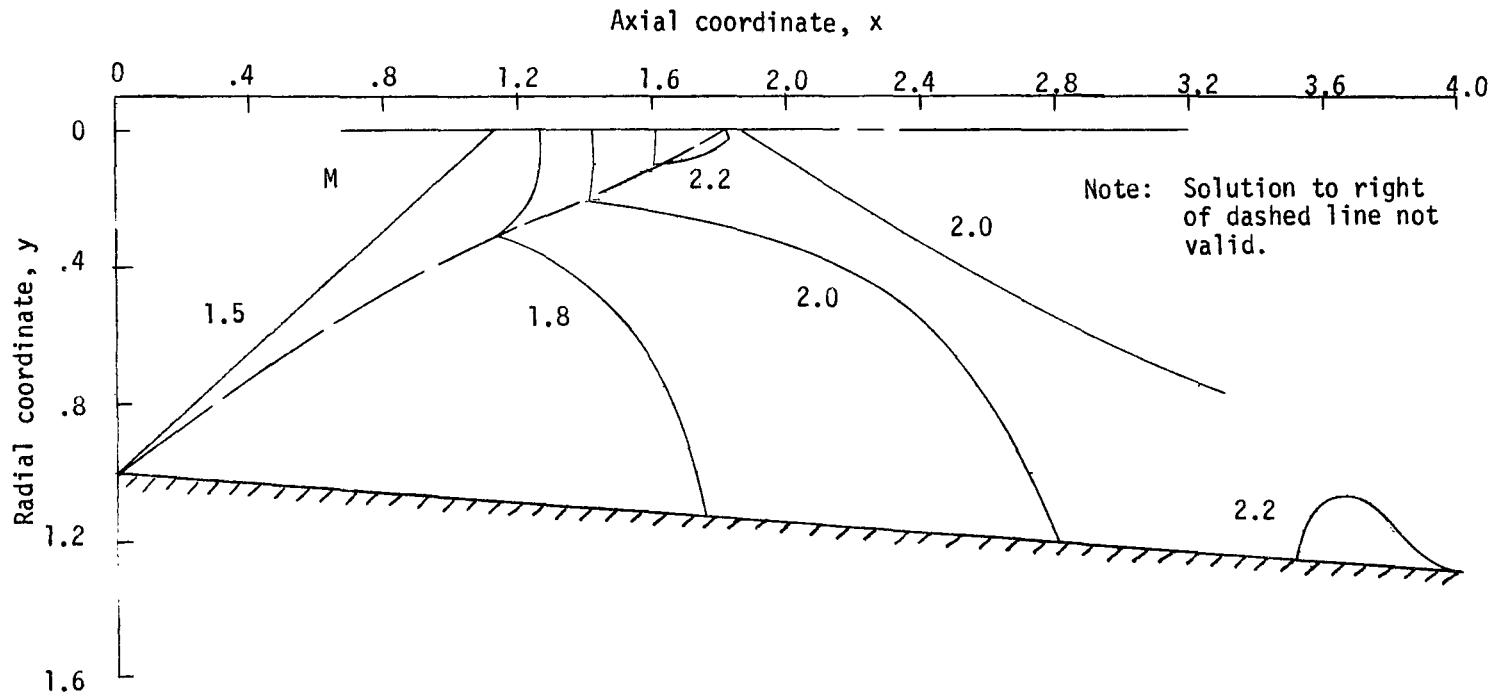

Figure 3.- Constant Mach number contours with shock present for conical nozzle with $M_i = 1.5$ and $\theta_1 = 4.14^o$.

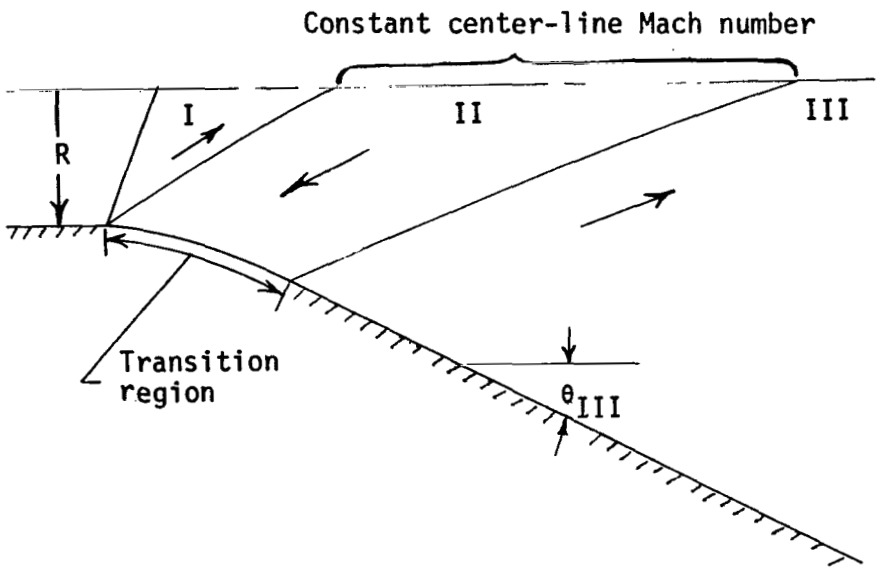

Figure 4.- Illustration of computing regions for shock elimination scheme.

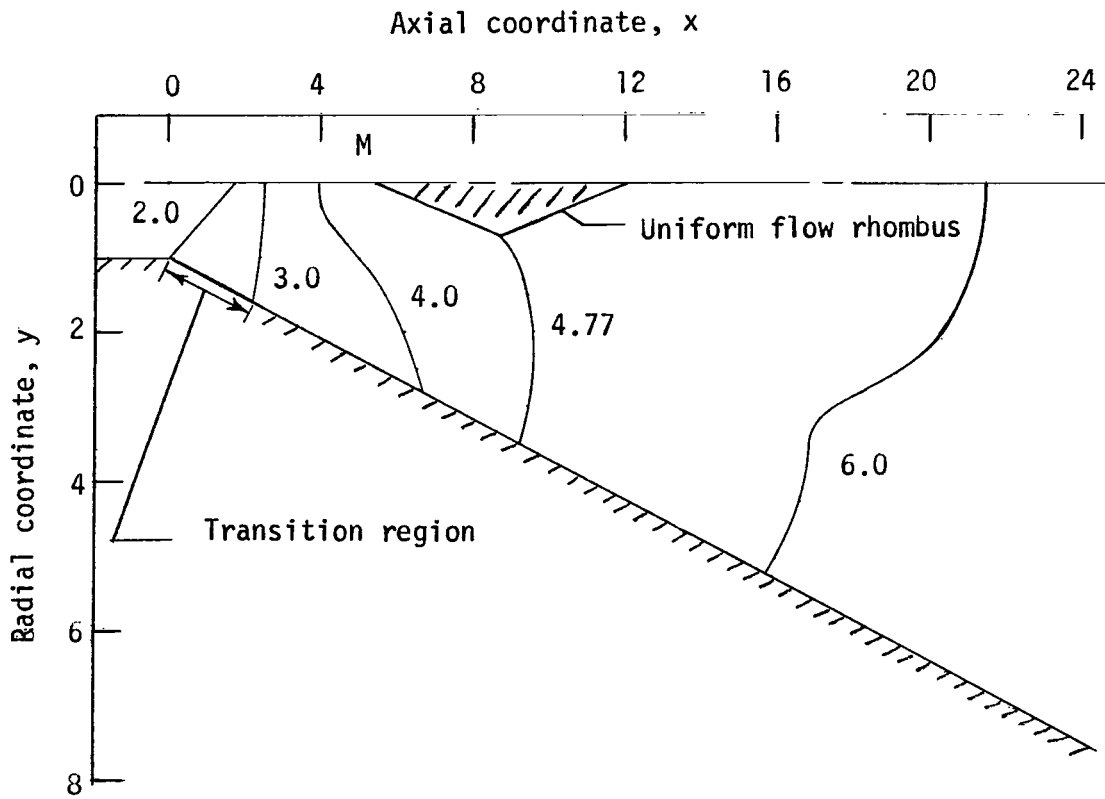

Figure 5.- Constant Mach number contours with shock eliminated for $M_i = 2.0$, $\theta_I = 9.58^0$, and $\theta_{III} = 15.15^0$.

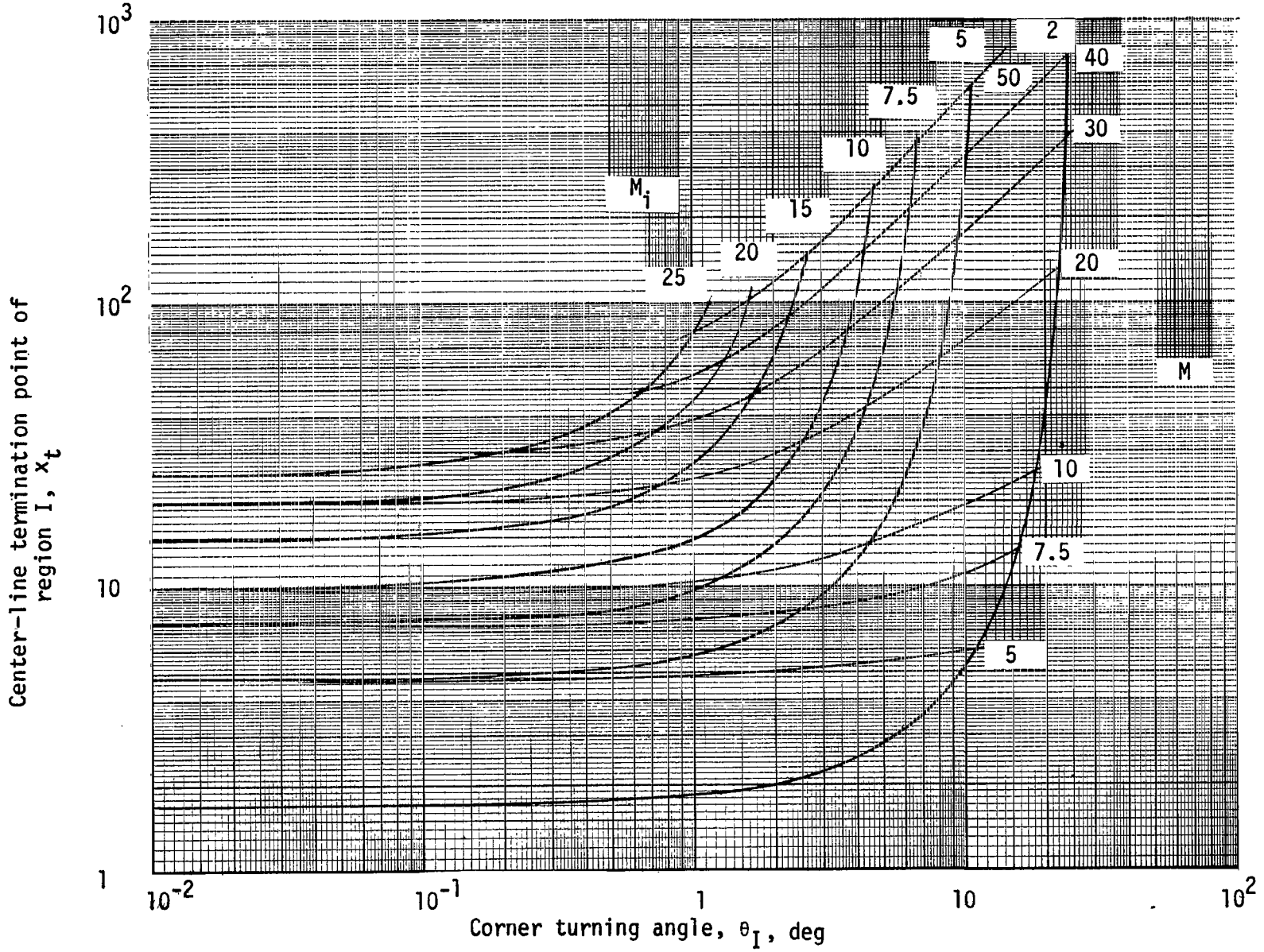

Figure 6.- Operating chart for center-line flow of region I (axisymmetric corner expansion).

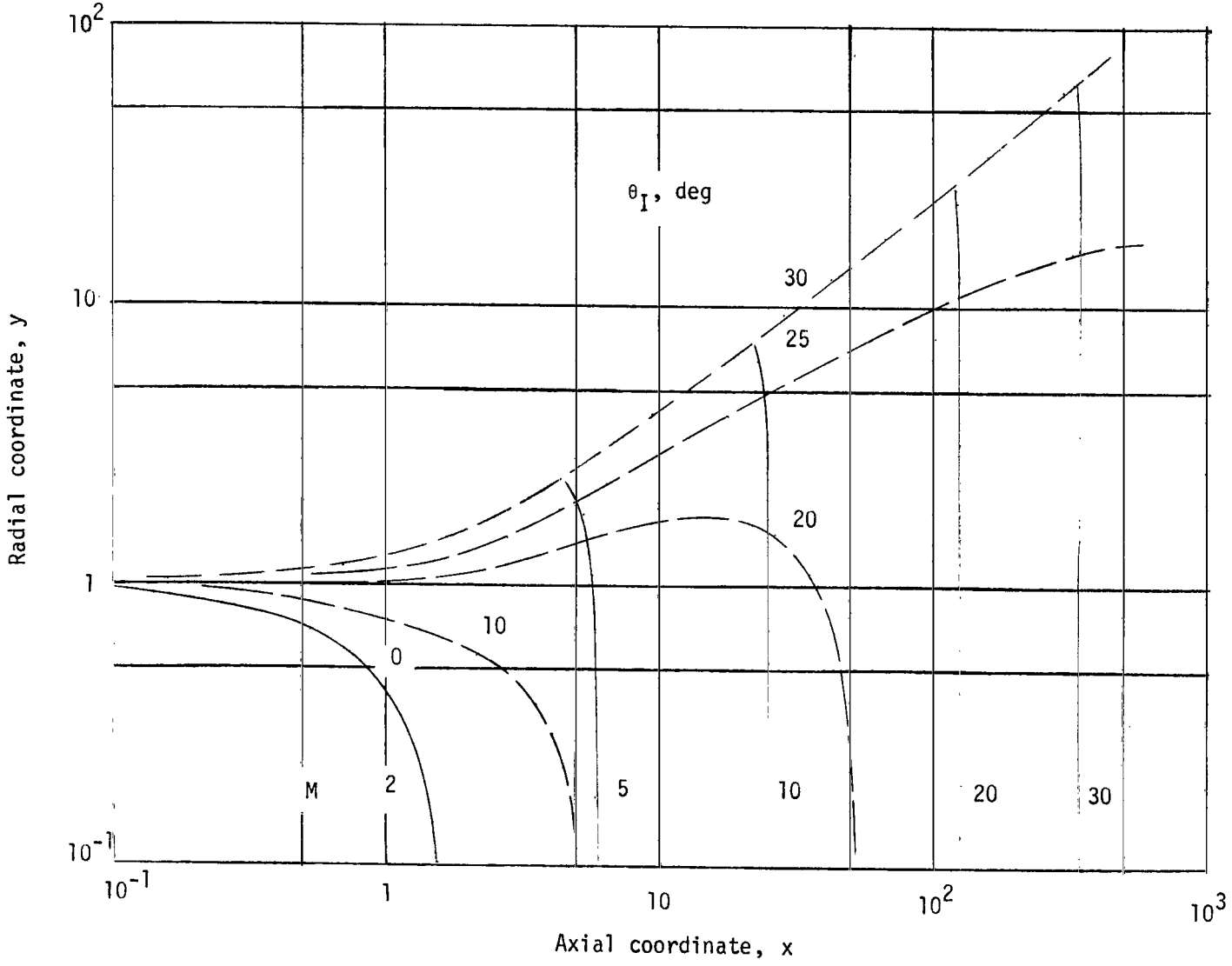

(a) $M_i = 2.0$.

Figure 7.- Constant Mach number contours within boundaries of region I.

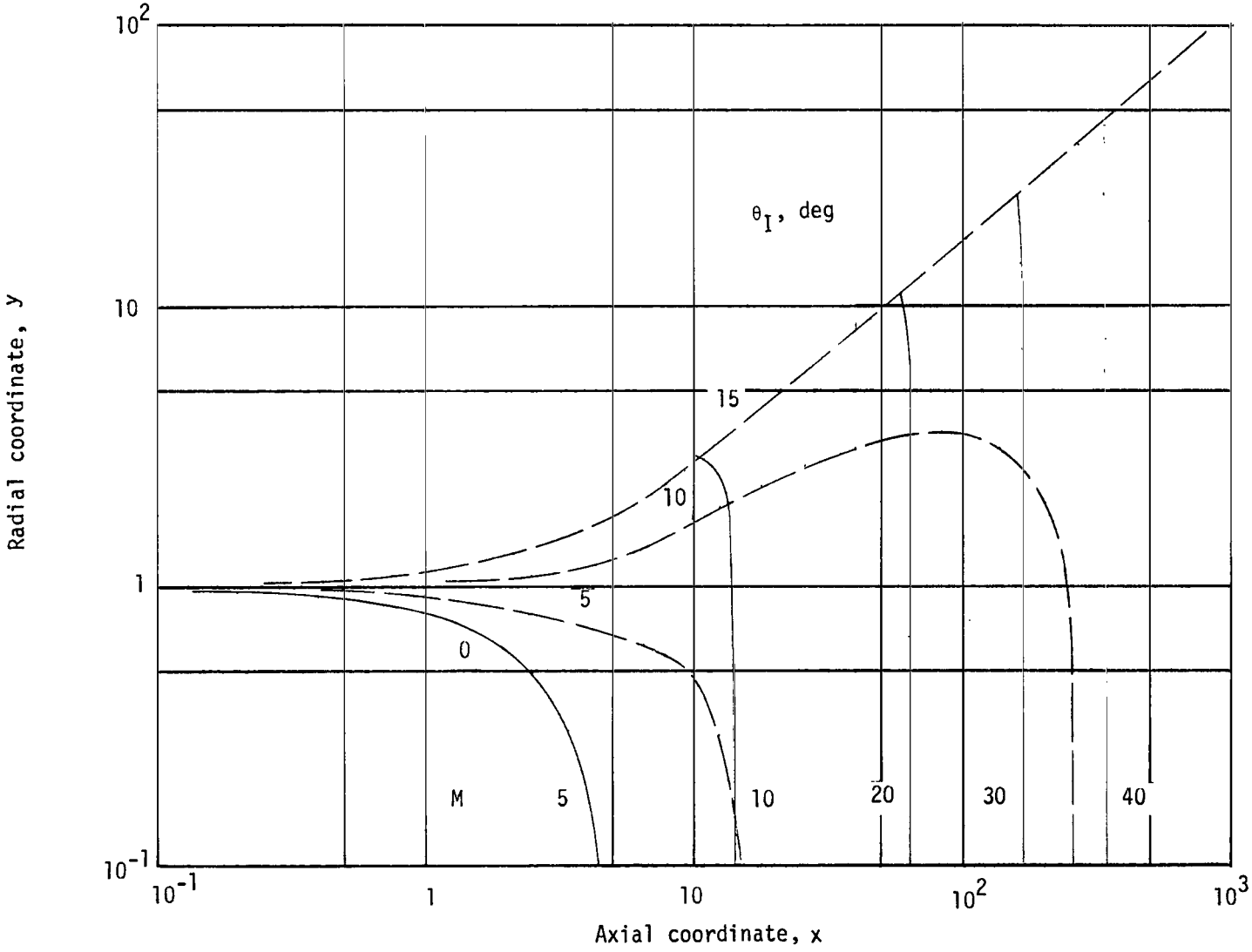

(b) $M_i = 5.0$.

Figure 7.- Continued.

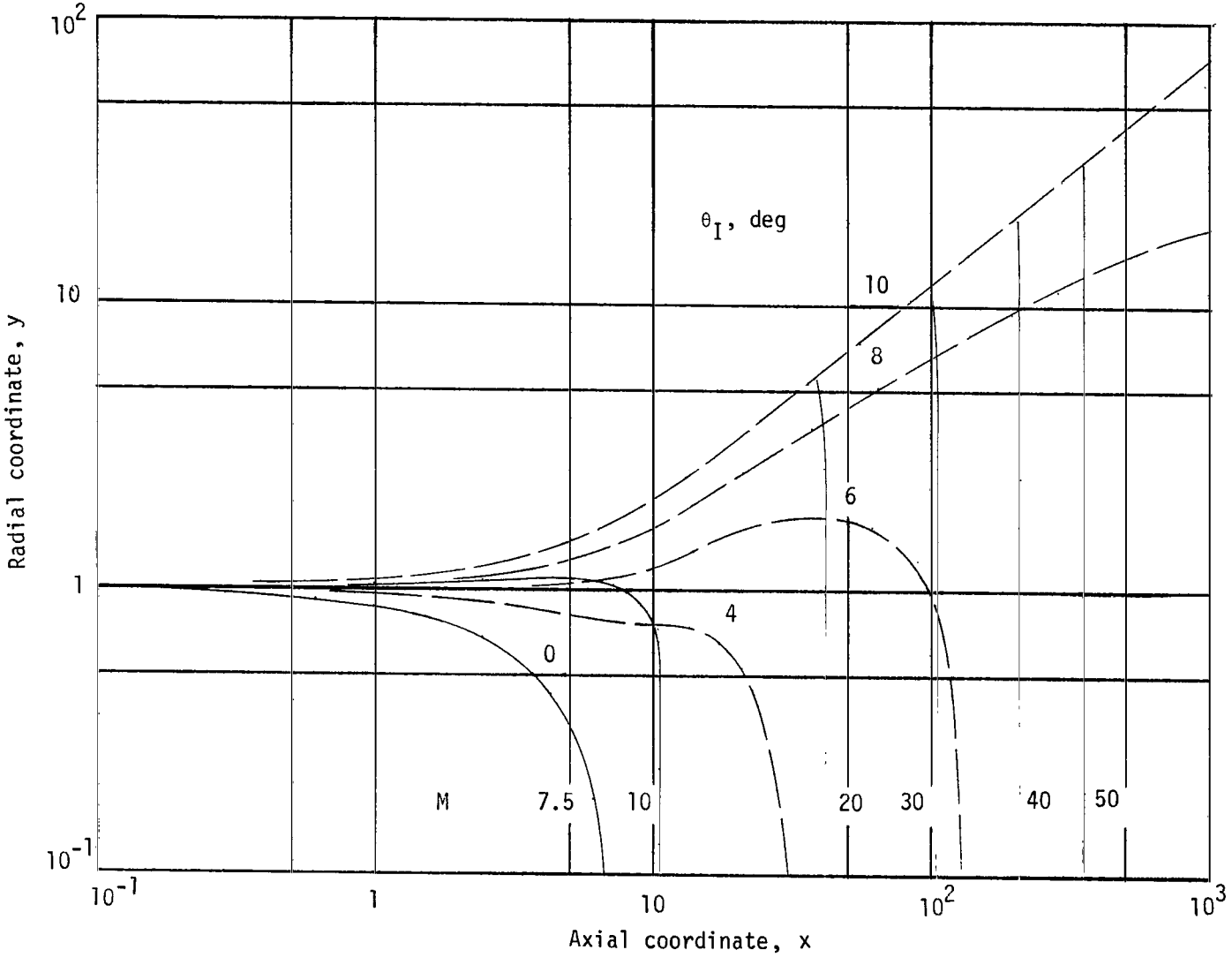

(c) $M_i = 7.5$.

Figure 7.- Continued.

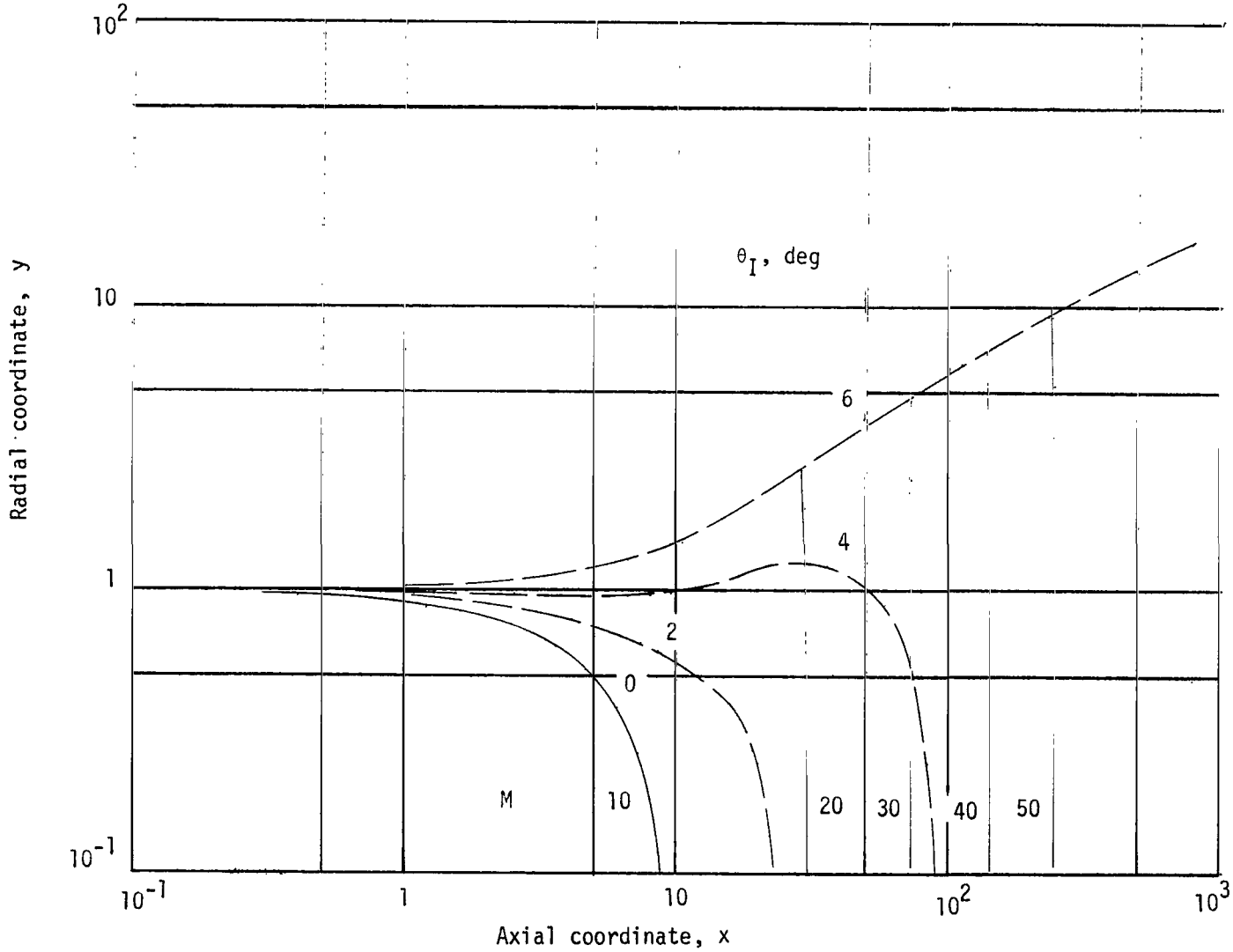

(d) M_j = 10.0.

Figure 7.- Continued.

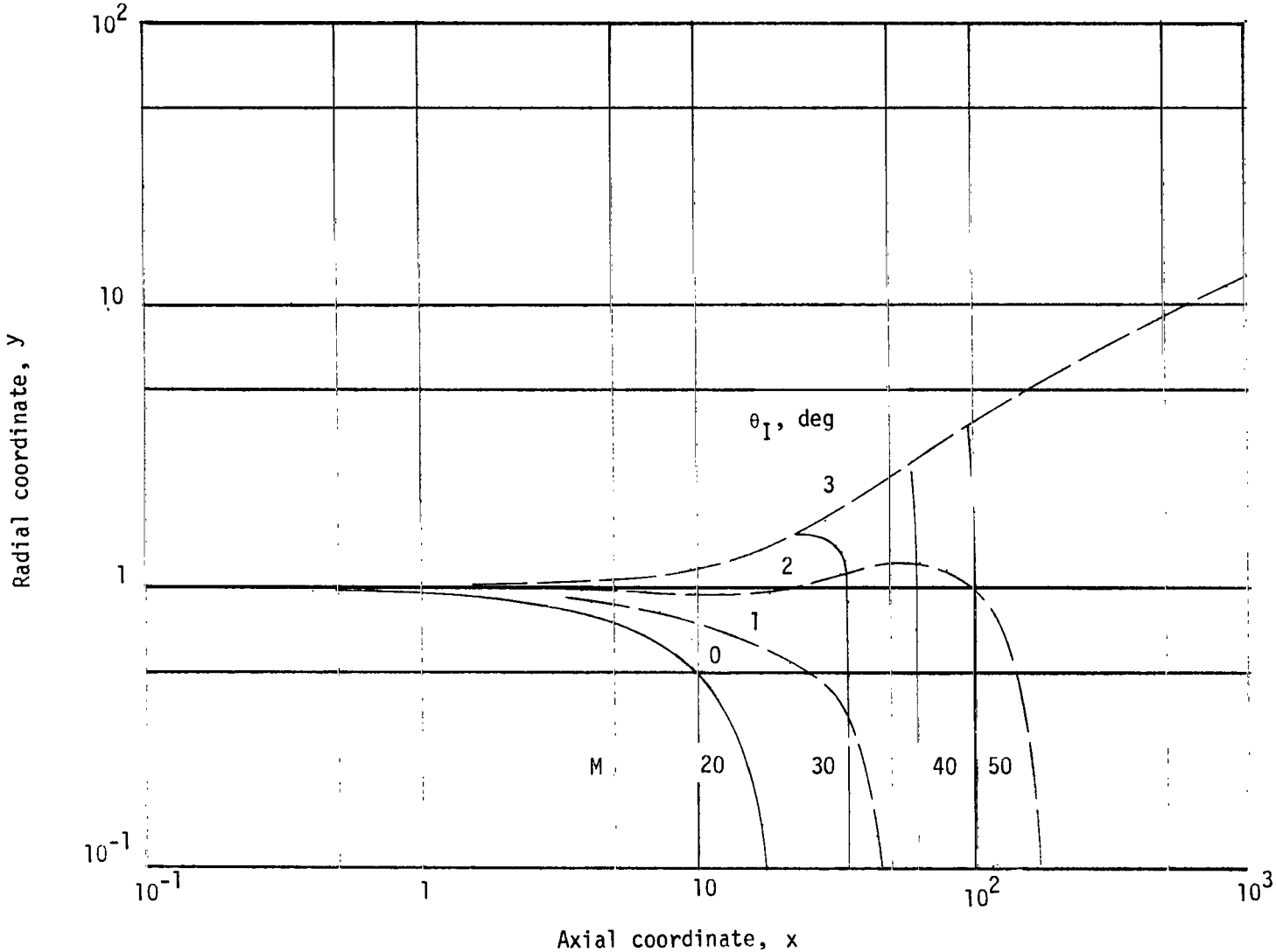

(e) $M_j = 20.0$.

Figure 7.- Concluded.

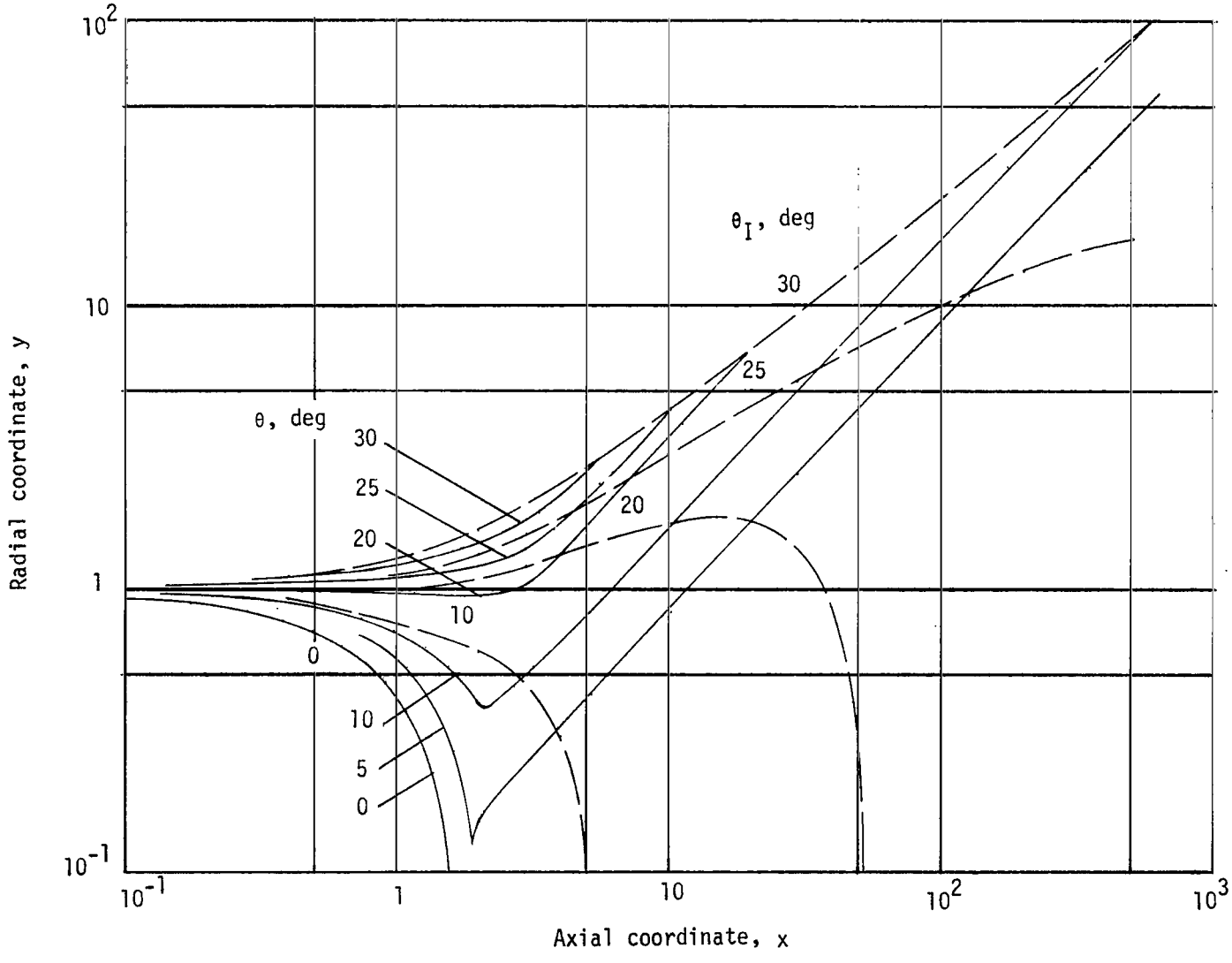

(a) $M_j = 2.0$.

Figure 8.- Constant-flow-inclination contours within boundaries of region I.

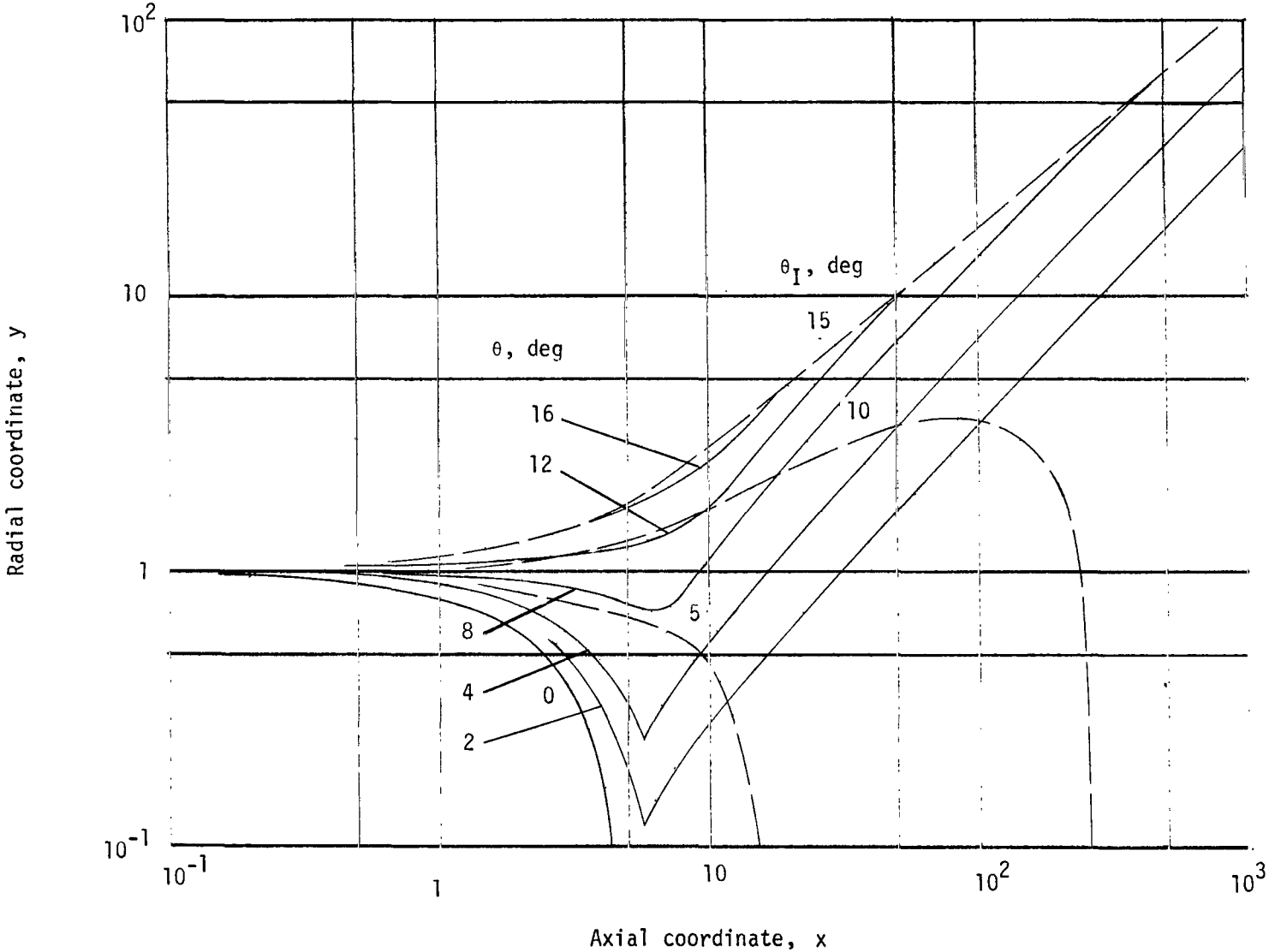

(b) M_j = 5.0.

Figure 8.- Continued.

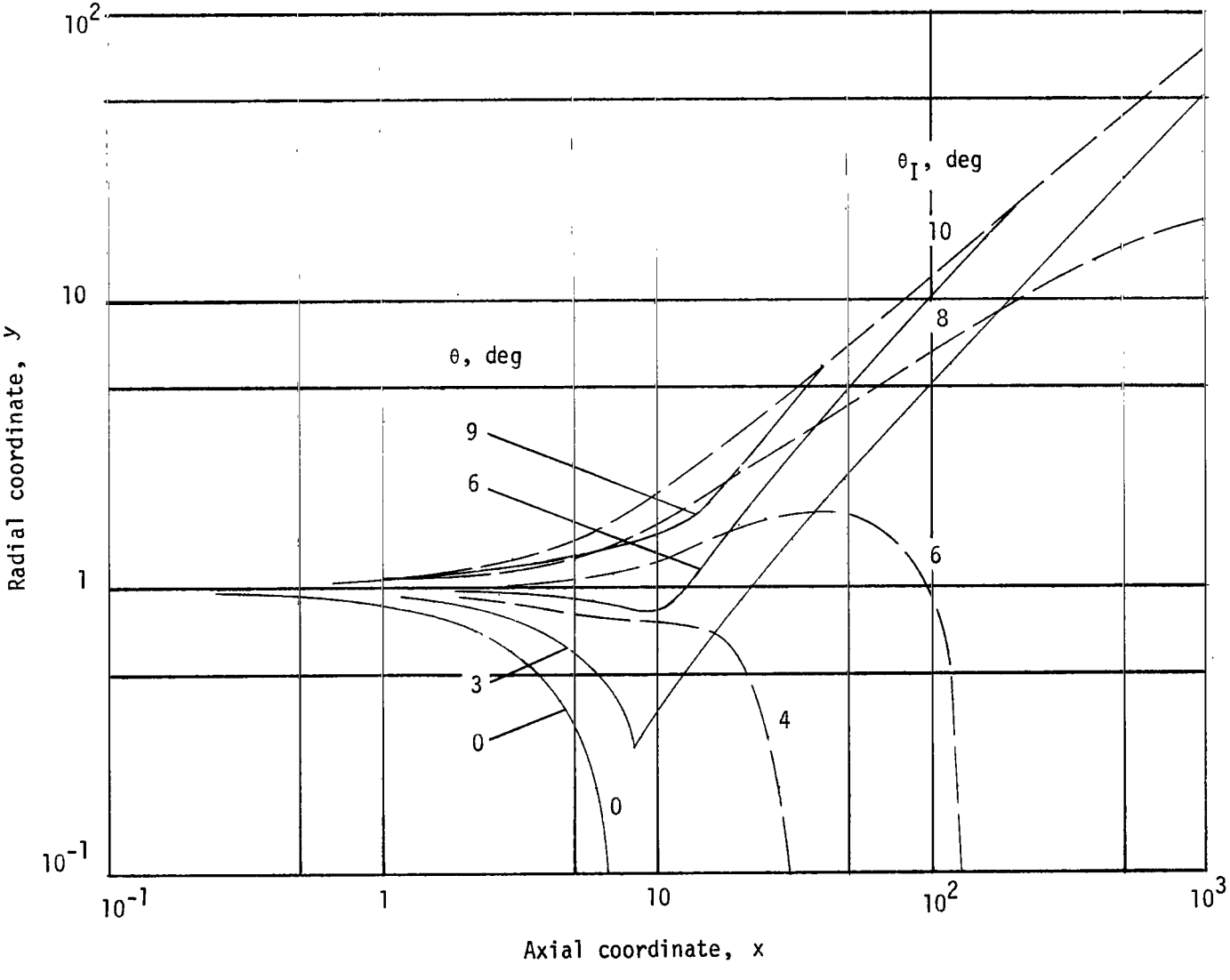

(c) $M_j = 7.5$.

Figure 8.- Continued.

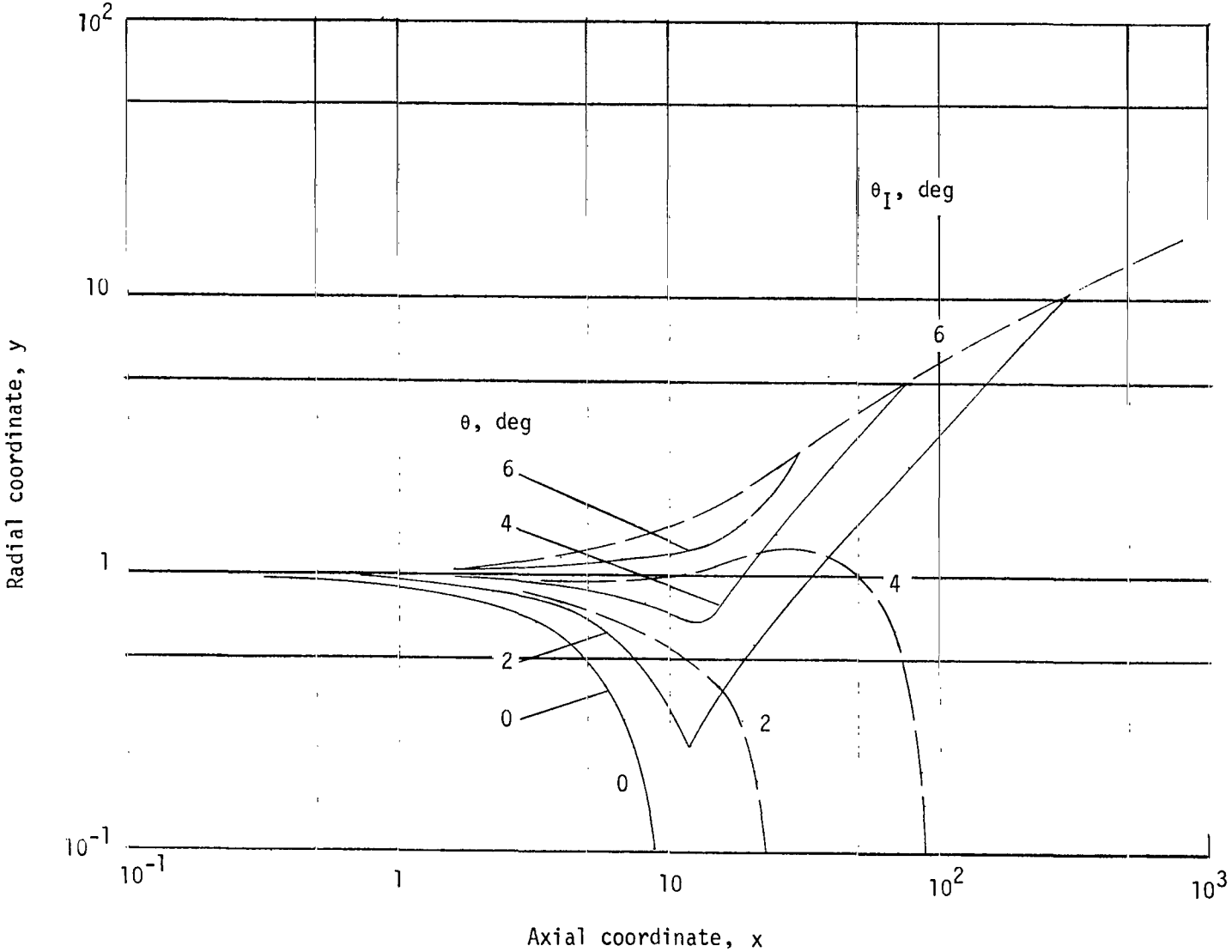

(d) M_j = 10.0.

Figure 8.- Continued.

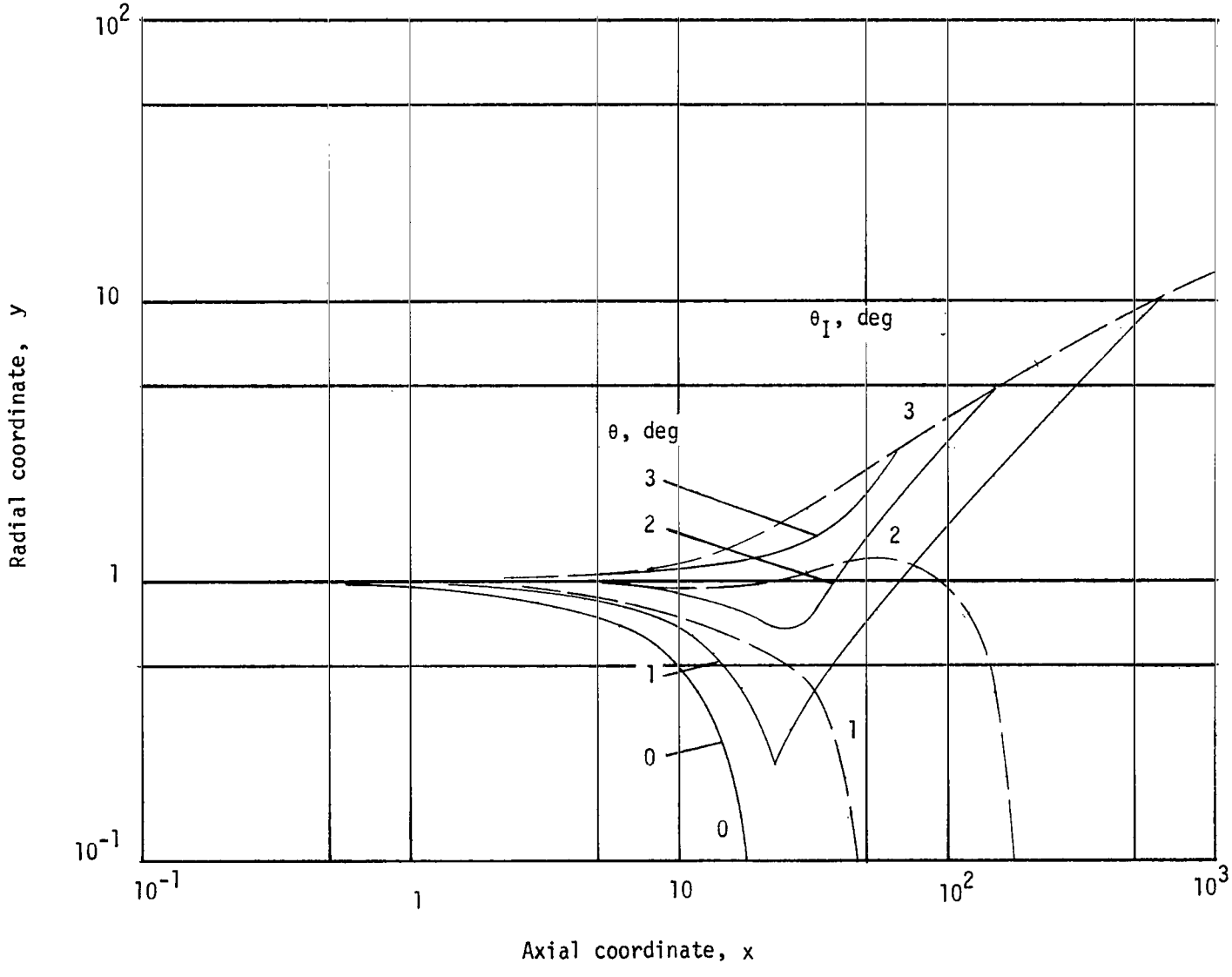

(e) M_j = 20.0.

Figure 8.- Concluded.

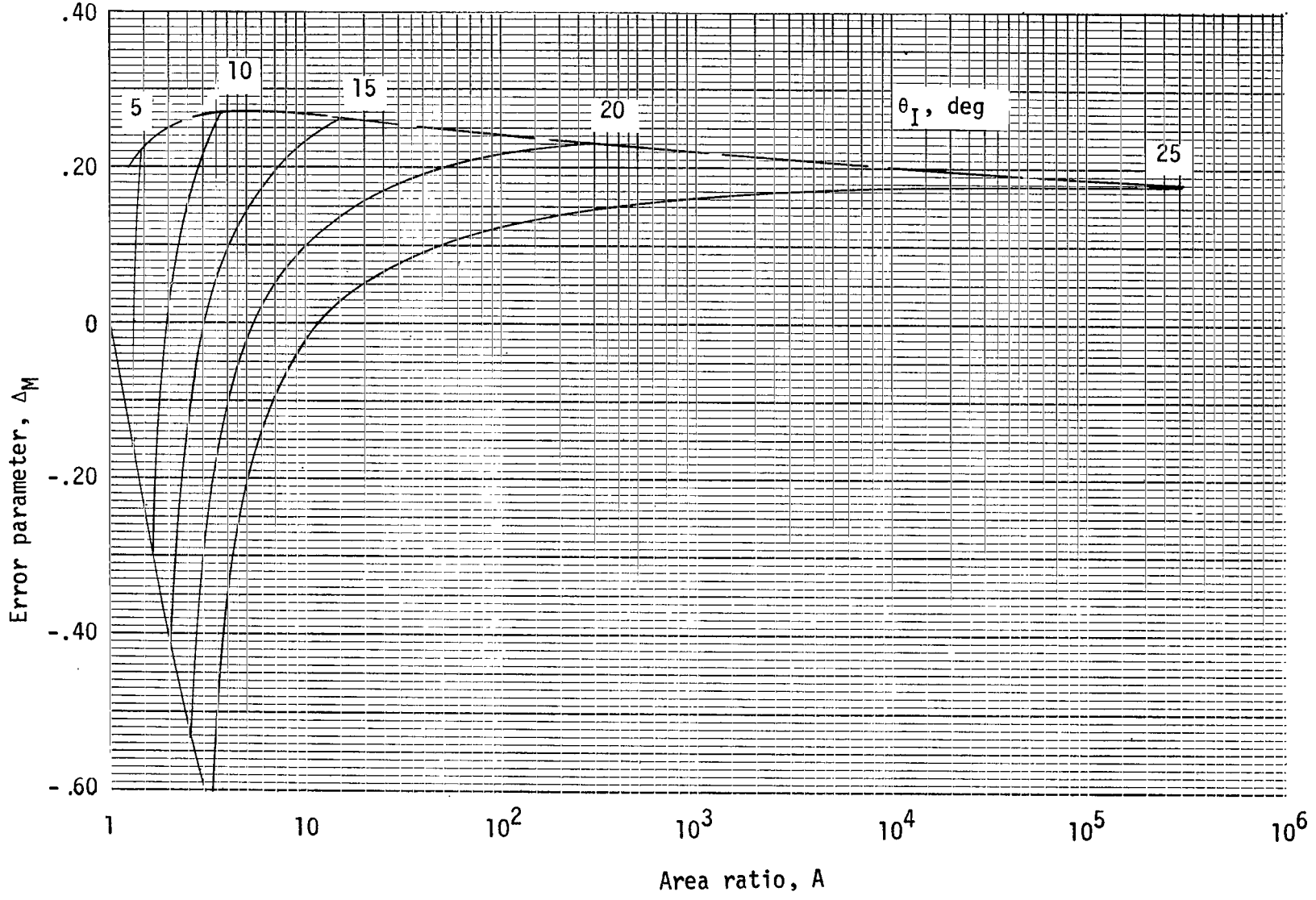

(a) $M_i = 2.0$.

Figure 9.- Error in center-line Mach number due to one-dimensional analysis in region I.

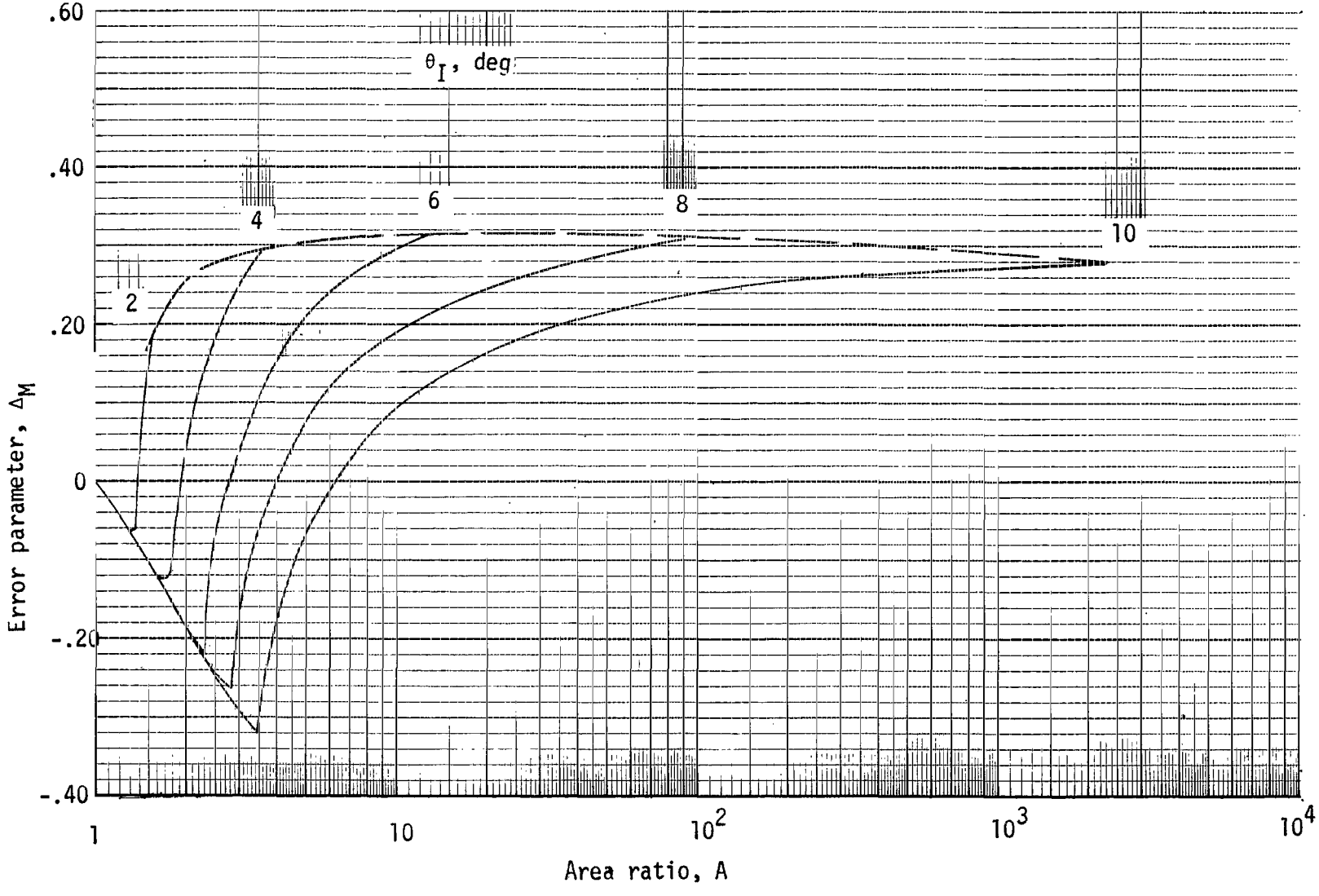

(b) $M_i = 5.0$.

Figure 9.- Continued.

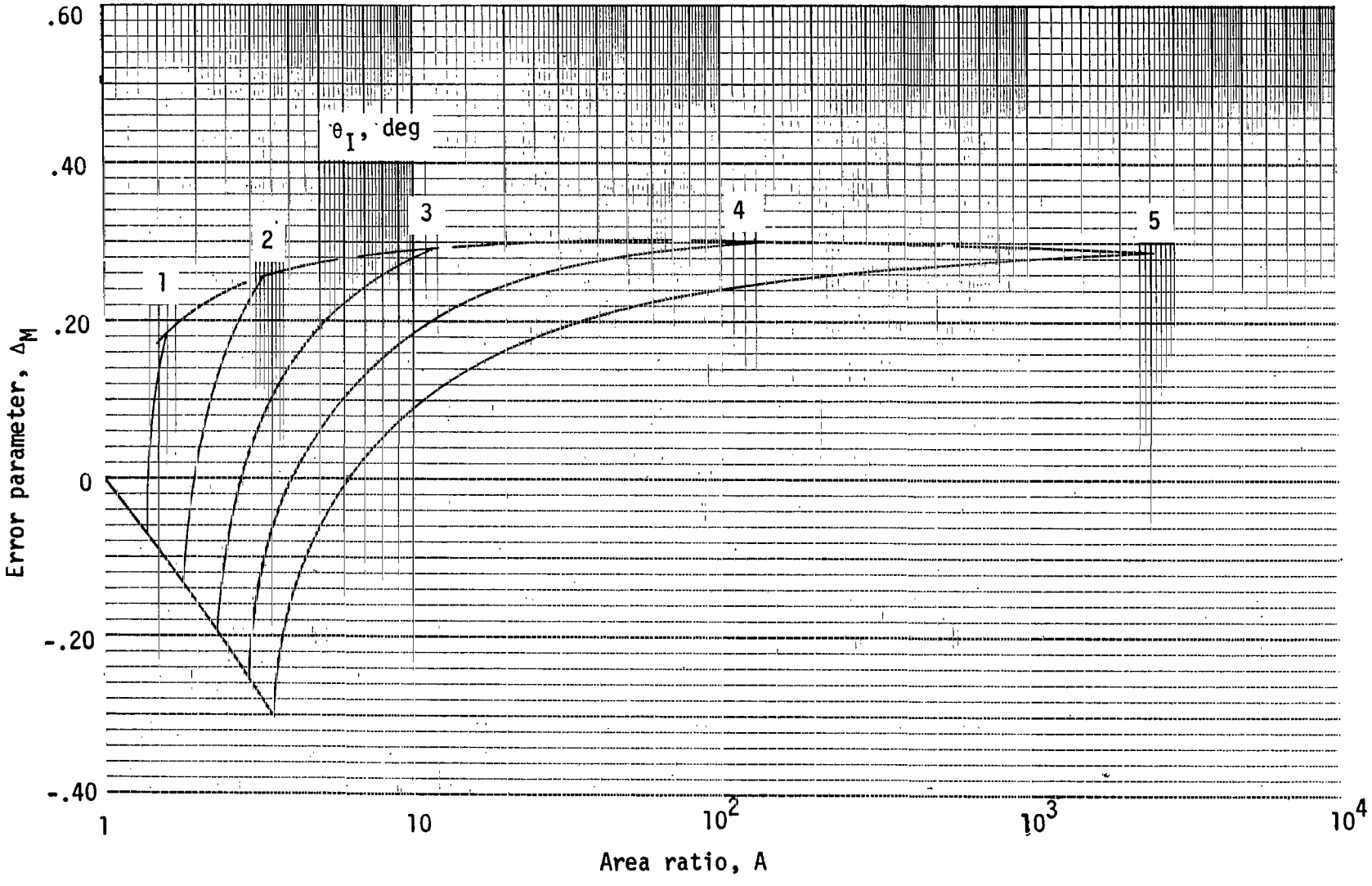

(c) M_j = 10.0.

Figure 9.- Continued.

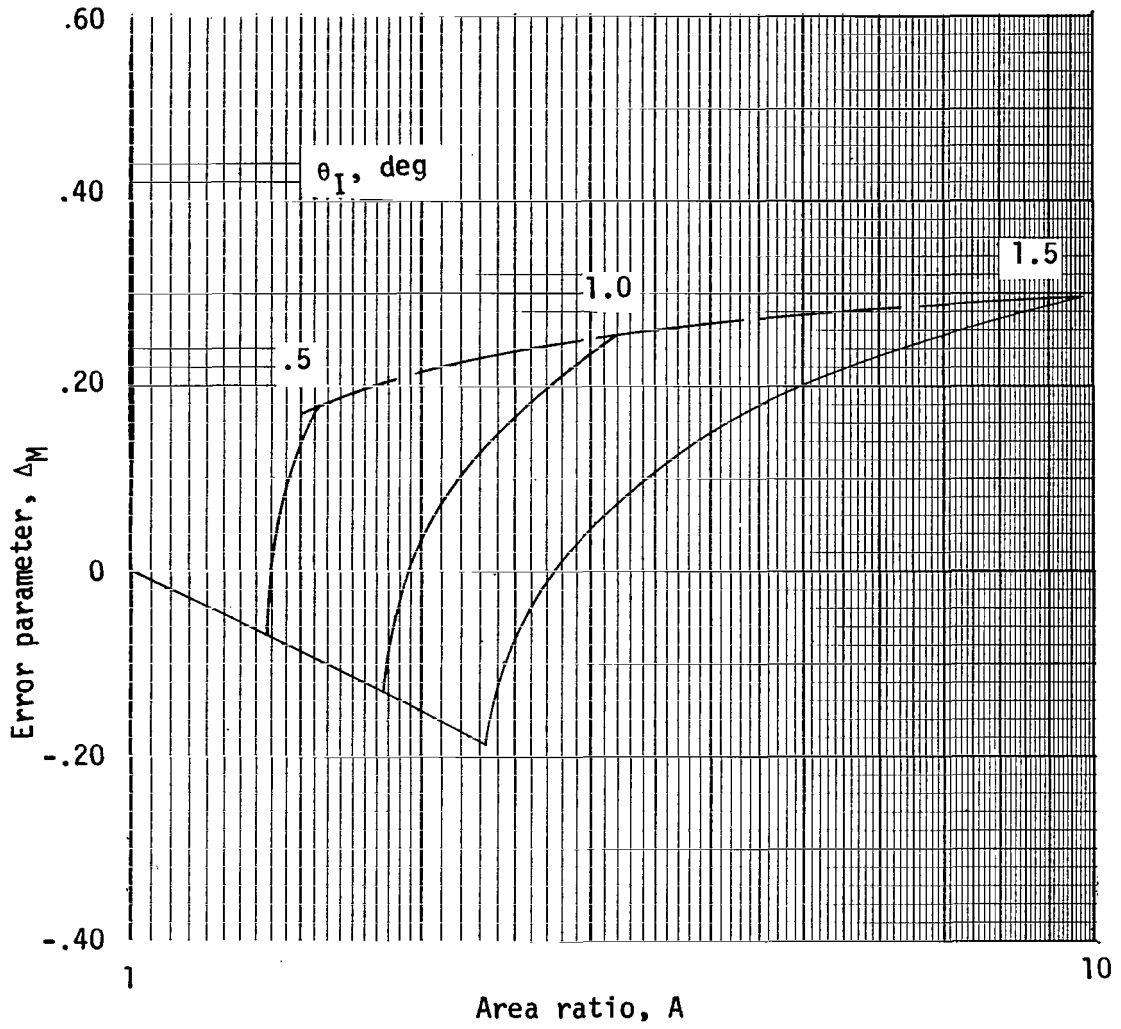

(d) M_i = 20.0.

Figure 9.- Concluded.

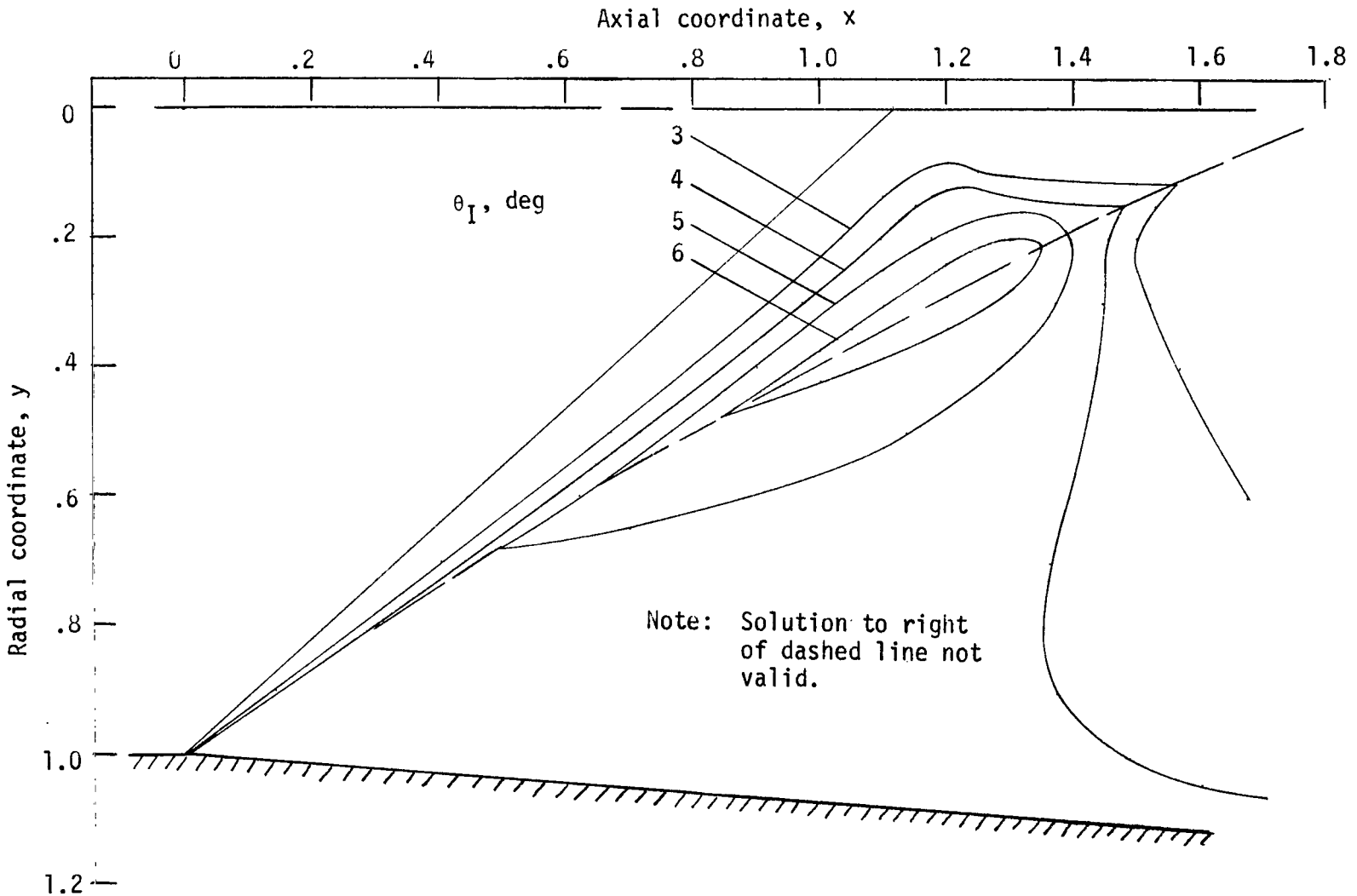

Figure 10.- Constant flow inclination contours with shock present for conical nozzle with $M_i = 1.5$, and $\theta_I = 4.14^0$.

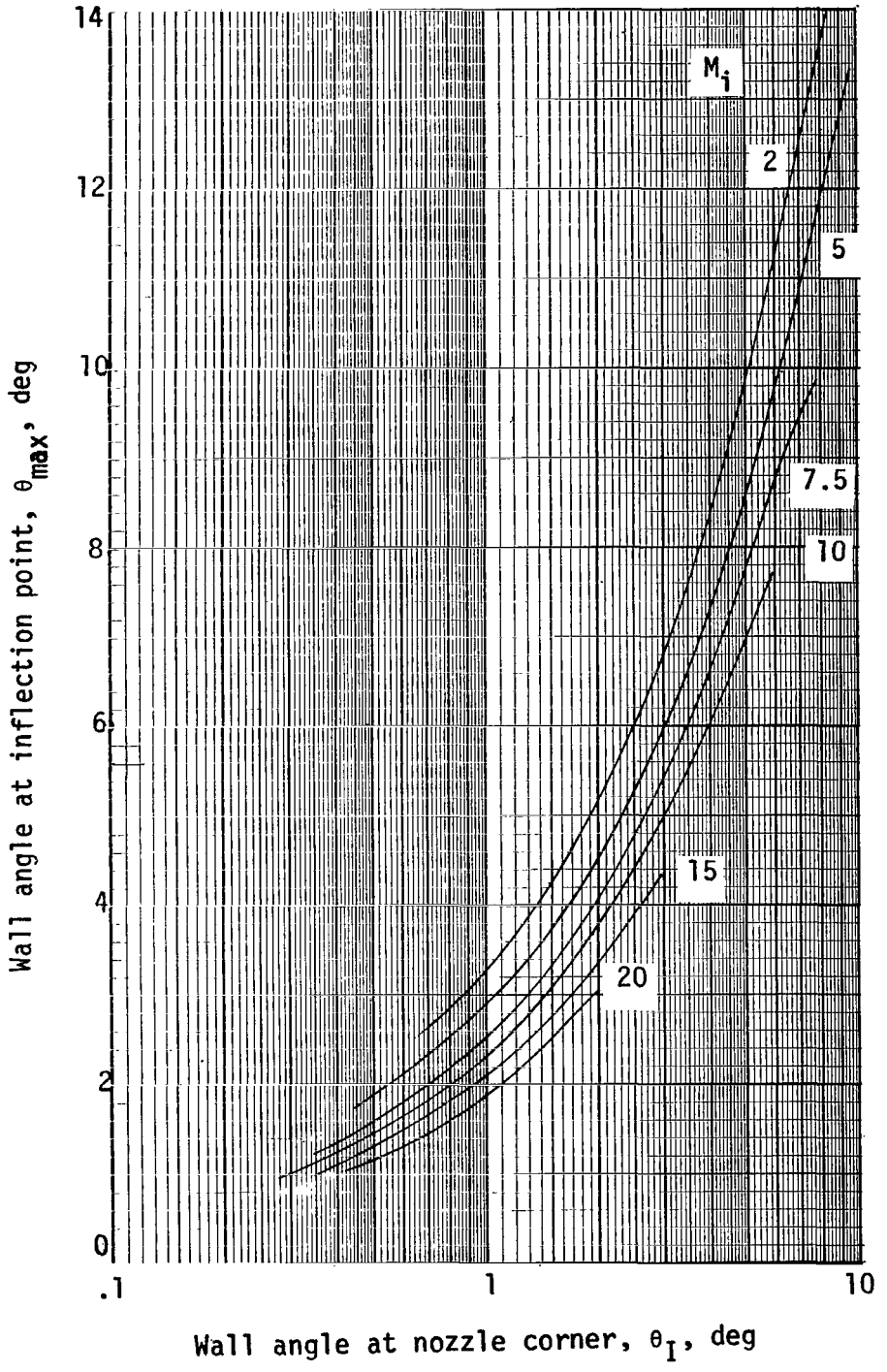

Figure 11.- Variation of θ_{max} with θ_I and M_i.

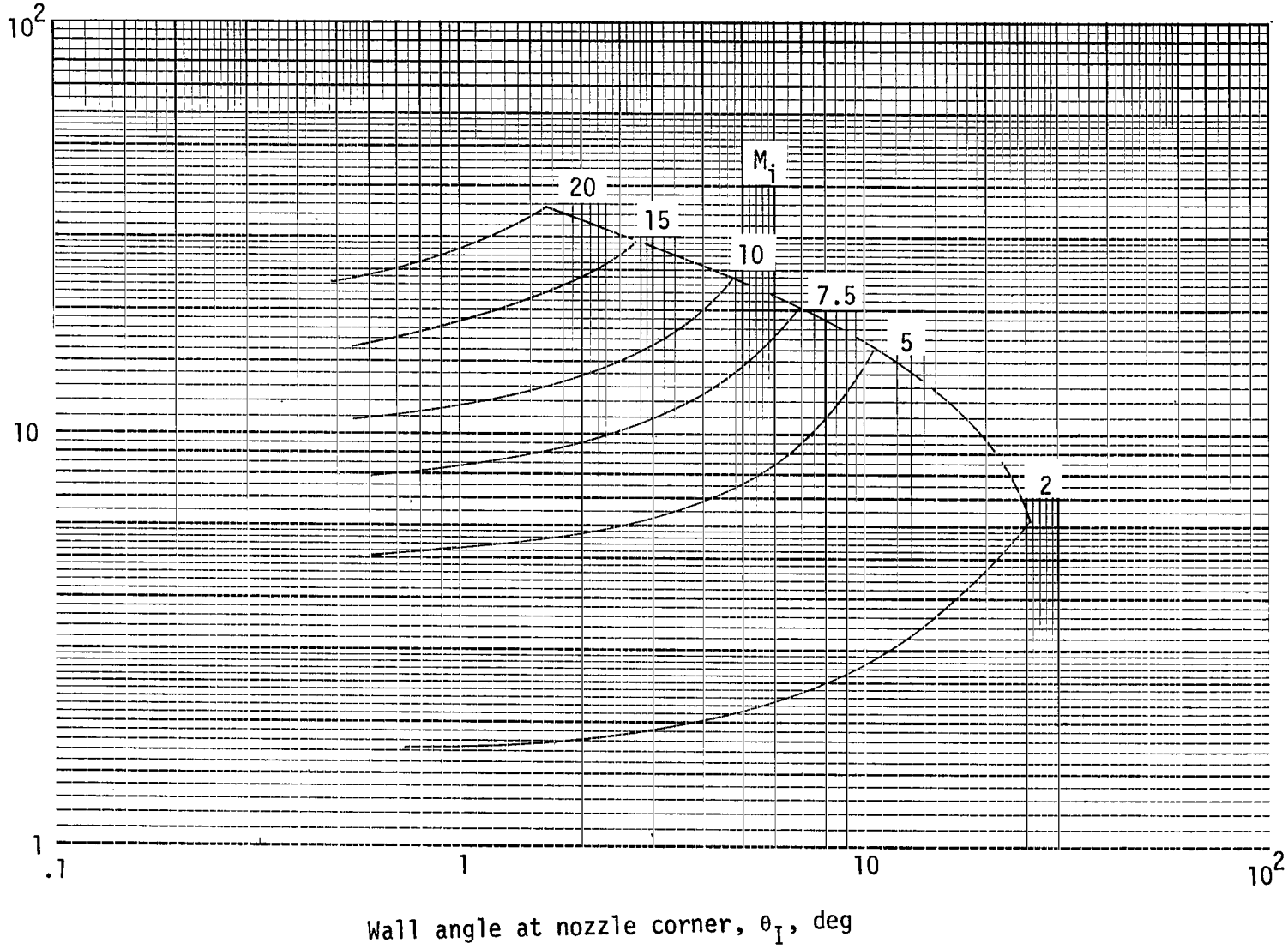

Figure 12.- Variation of x_{max} with θ_I and M_i.

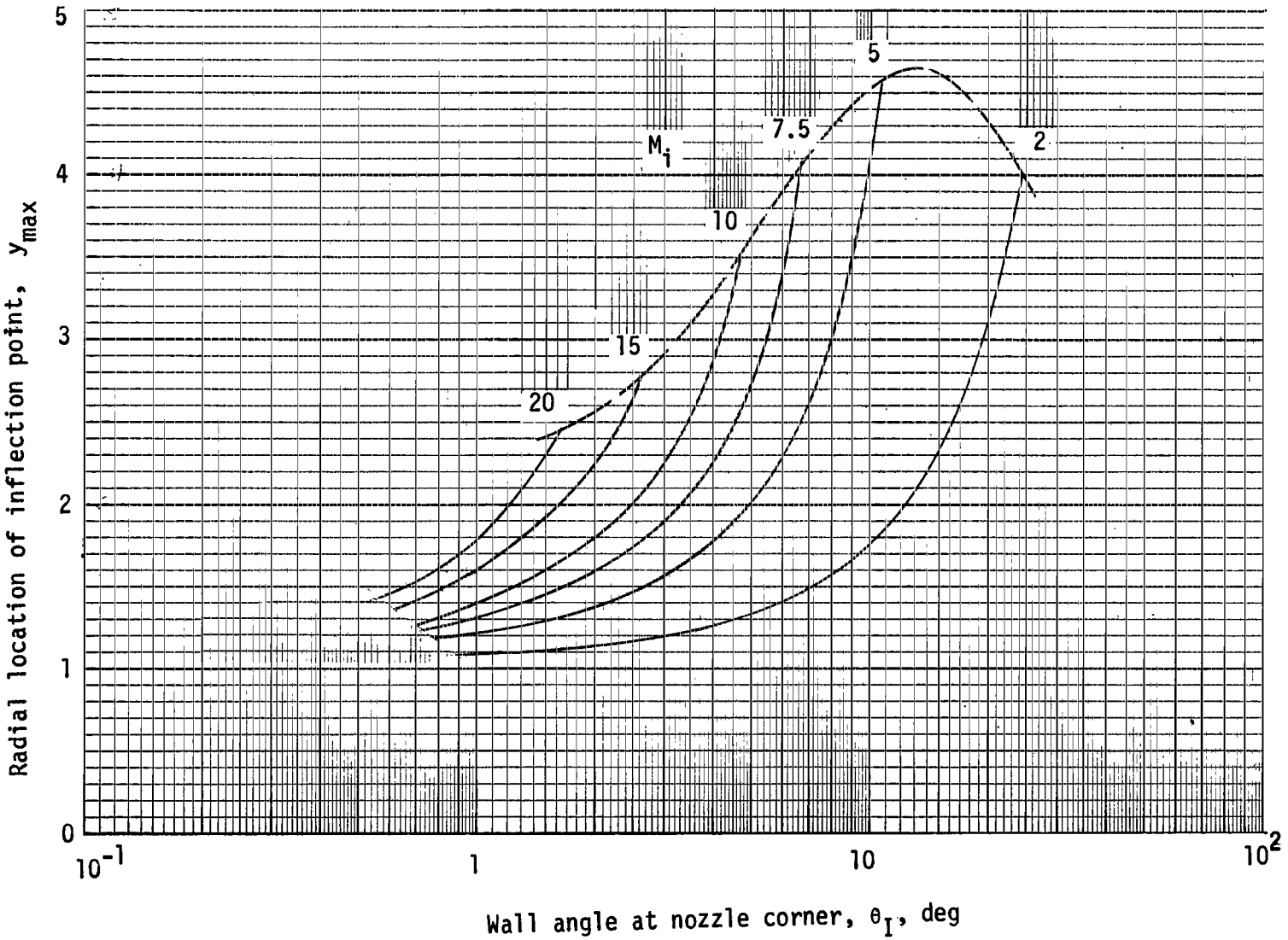

Figure 13.- Variation of y_{max} with θ_I and M_i.

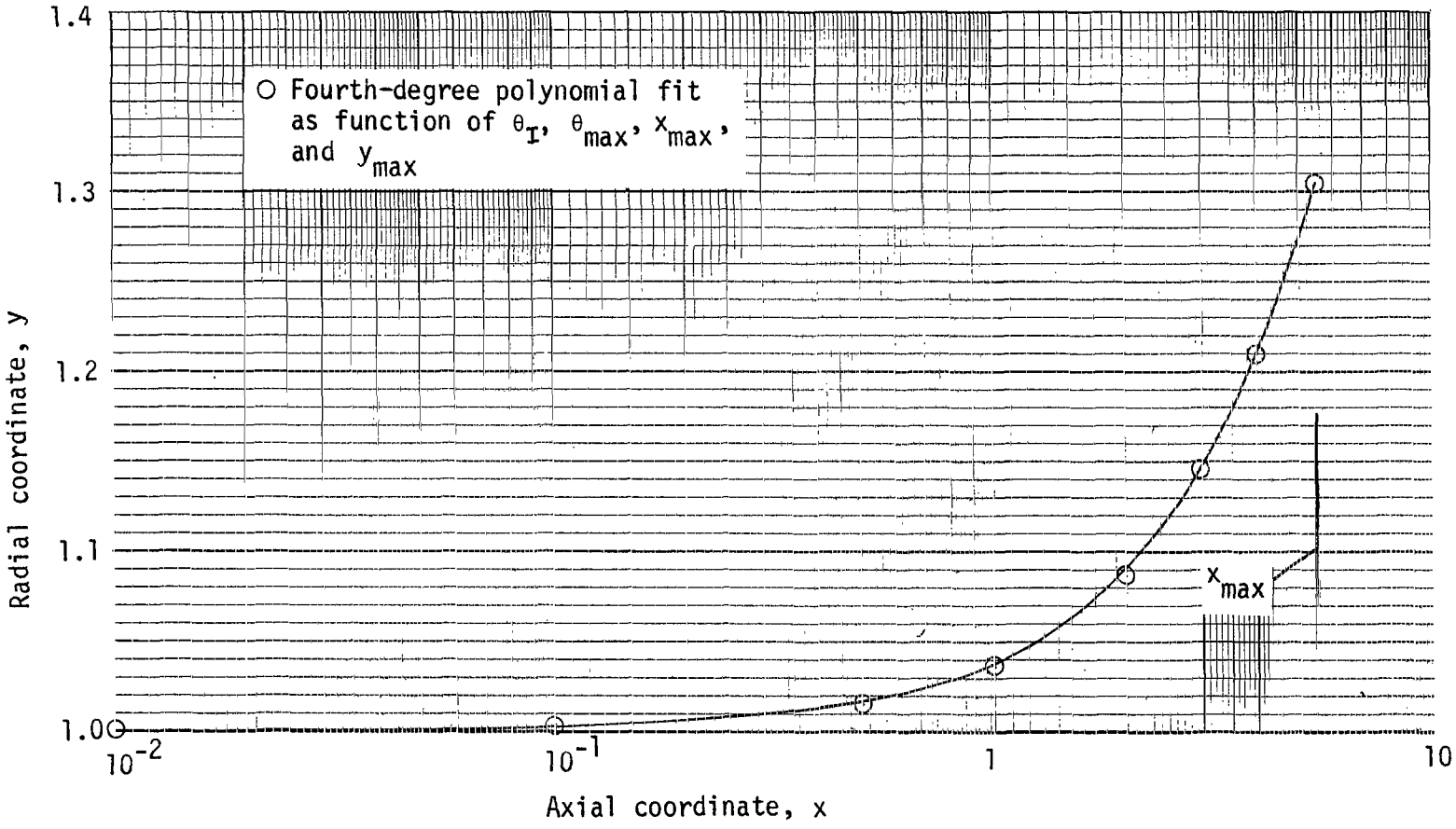

Figure 14.- Typical transition contour for $M_i = 5.0$, $\theta_I = 1.570^0$ and $\theta_{max} = 3.710^0$.

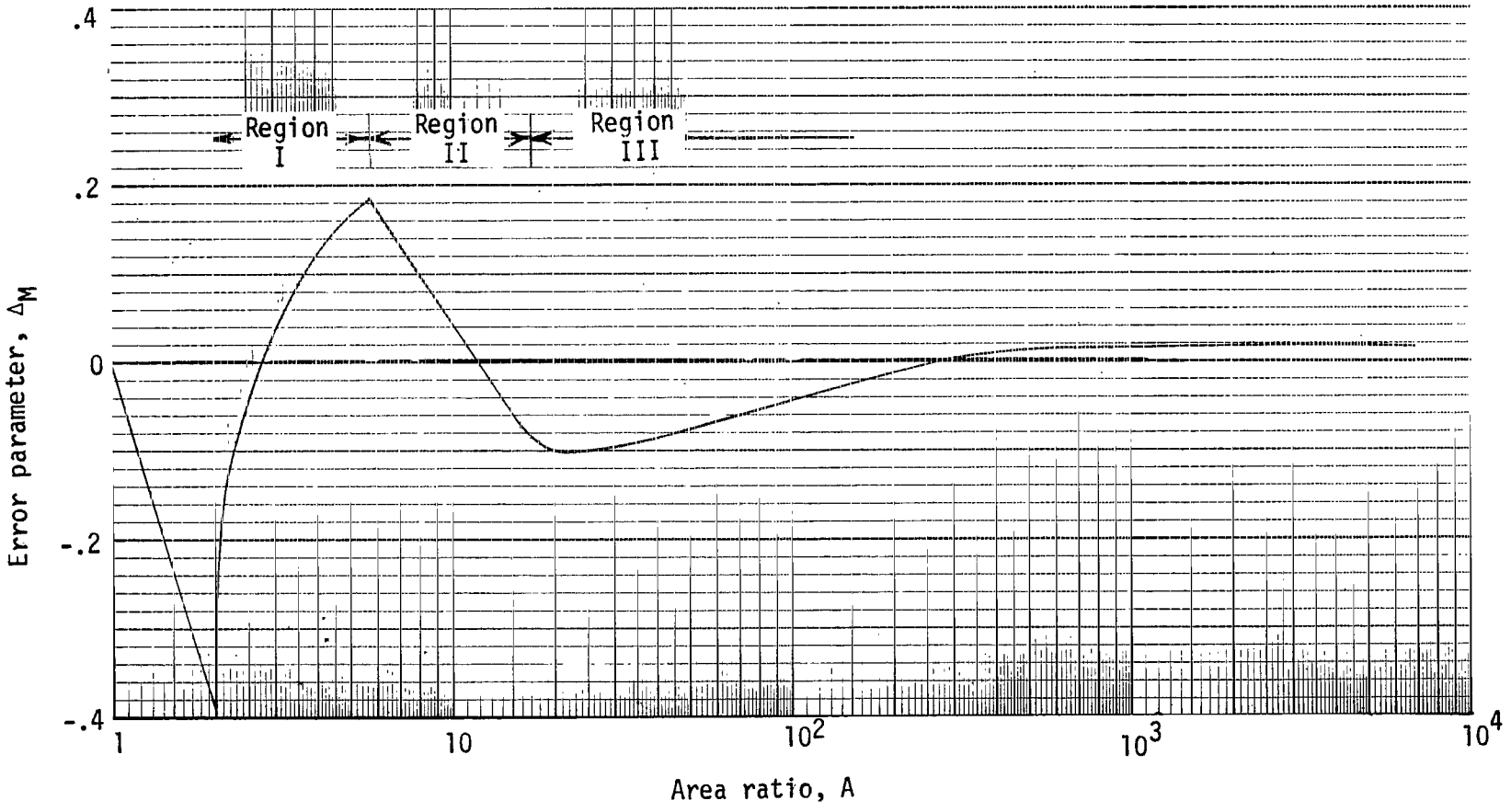

Figure 15.- Center-line variation of Δ_M in a shock-free nozzle with $M_i = 2.0$, $\theta_I = 9.58^0$, and $\theta_{III} = 15.15^0$.

"The aeronautical and space activities of the United States shall be conducted so as to contribute . . . to the expansion of human knowledge of phenomena in the atmosphere and space. The Administration shall provide for the widest practicable and appropriate dissemination of information concerning its activities and the results thereof."

—NATIONAL AERONAUTICS AND SPACE ACT OF 1958

NASA SCIENTIFIC AND TECHNICAL PUBLICATIONS

TECHNICAL REPORTS: Scientific and technical information considered important, complete, and a lasting contribution to existing knowledge.

TECHNICAL NOTES: Information less broad in scope but nevertheless of importance as a contribution to existing knowledge.

TECHNICAL MEMORANDUMS: Information receiving limited distribution because of preliminary data, security classification, or other reasons.

CONTRACTOR REPORTS: Technical information generated in connection with a NASA contract or grant and released under NASA auspices.

TECHNICAL TRANSLATIONS: Information published in a foreign language considered to merit NASA distribution in English.

TECHNICAL REPRINTS: Information derived from NASA activities and initially published in the form of journal articles.

SPECIAL PUBLICATIONS: Information derived from or of value to NASA activities but not necessarily reporting the results of individual NASA-programmed scientific efforts. Publications include conference proceedings, monographs, data compilations, handbooks, sourcebooks, and special bibliographies.

Details on the availability of these publications may be obtained from:

SCIENTIFIC AND TECHNICAL INFORMATION DIVISION

NATIONAL AERONAUTICS AND SPACE ADMINISTRATION

Washington, D.C. 20546